

# FT-ICR Studies of Solvation Effects in Ionic Water Cluster Reactions

Gereon Niedner-Schatteburg and Vladimir E. Bondybey\*

*Institut für Physikalische und Theoretische Chemie, Technische Universität München, 85747 Garching, Germany*

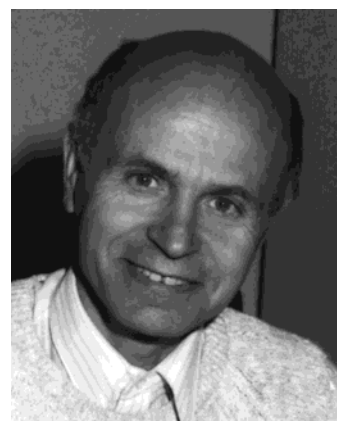
Received April 4, 2000

## Contents

I. Introduction	4059
II. Experimental Techniques for Cluster Studies	4060
A. Methods for Generating Water Clusters	4060
B. Techniques for Studies of Ion–Neutral Reactions	4061
III. Hydrated Ions, their Stability and Structure	4064
A. Stability and Fragmentation of Water Clusters	4066
B. Infrared-Induced Fragmentation	4067
C. “Magic” Cluster Sizes	4069
D. Effect of the Central Ion	4070
E. Ions in Pure Water and the Structure of the Aqueous Proton	4071
IV. Water Clusters as a Medium for Aqueous Reactions	4073
A. Reduction–Oxidation Processes in Water Clusters	4074
B. Multiply Ionized Clusters	4075
C. Ionic Dissolution, Neutralization, and Precipitation Reactions in Water Clusters	4075
D. Acid and Basic Clusters and Catalytic Processes	4077
E. Reactions of Water Clusters with Polar Organic Molecules: Hydrophobic and Hydrophilic Interactions	4078
F. Water Clusters as Model Systems for Atmospheric Reactions	4079
G. Selected other Reactions of Water Clusters and Hydrated Ions	4083
V. Summary	4083
VI. References	4084



Gereon Niedner-Schatteburg studied physics at the Universität Göttingen and worked on crossed-beam proton molecule scattering in the group of J. Peter Toennies, obtaining his doctoral degree in 1988. During a postdoctoral stay in the group of Y. T. Lee at the University of California, Berkeley, he worked on the IR spectroscopy of molecular cluster ions. In 1990 he joined the group of V. E. Bondybey at the Technische Universität München and worked on the reactivity of charged metal clusters and ionic water clusters by means of an FT-ICR instrument. In 1997 he achieved his Habilitation degree in Chemistry. Effective October 2000, he has accepted the call to a chair in physical chemistry at the Universität Kaiserslautern.



Vladimir E. Bondybey studied at the Charles University in Prague, Czech Republic, and University of Rostock, East Germany. From 1969 he attended the University of California in Berkeley, working in the area of matrix isolation, and obtaining his PhD with George Pimentel in 1972. From 1973 until 1988 he was a Distinguished Member of Technical Staff at the AT&T Bell Laboratories, doing research in various areas of physical chemistry and spectroscopy. After a few years as a Professor at The Ohio State University, he accepted in 1989 a chair in physical chemistry at the Technical University of Munich. Since 1997 he also is an adjunct professor at the University of California, Irvine.

## I. Introduction

In recent years there has been a considerable interest in the structure, dynamics, and other properties of water and neutral water clusters. This has been clearly evidenced by a number of conferences, symposia, books, and workshops dedicated to these topics.<sup>1–8</sup> The interest is also not surprising since water is doubtless the most important liquid on earth. It is an excellent solvent with a number of interesting properties, and really “pure”, neutral water is actually not easy to come by; one mostly encounters it “dirty”, with other substances dissolved in it. Thus, 93% of the surface water on earth is in the oceans, which are far from pure and strictly

speaking also far from neutral, since they contain considerable quantities of dissolved matter, mainly in ionic form. Thus, for 1000 molecules of seawater,

\* Author to whom correspondence should be addressed. E-mail: bondybey@uci.edu.

there are some 10  $\text{Cl}^-$ , chloride ions, 9  $\text{Na}^+$  ions, an  $\text{Mg}^{2+}$  ion, and in fact, most elements of the periodic table are well represented. It is perhaps interesting to note that oceans contain more than  $10^{13}$  kilograms of gold.

Water is also the solvent of life, and most biological processes are unthinkable without it. However, again, water in biological systems is anything but pure. It contains numerous dissolved ions of both negative and positive charge, and gradients in the concentration of these ions play an important role in the passive transport of matter across semipermeable membranes in and out of living cells.<sup>9</sup> Even pure water, however, is not really "pure"; it will autoionize and contain a small but easily measurable concentration of ions,  $\text{H}_3\text{O}^+$  and  $\text{OH}^-$ , which in fact give it its electric conductivity and strongly affect its properties. In view of these observations, it is perhaps clear that also "dirty" water is not without interest. With the help of modern techniques, in the gas-phase clusters of water it is relatively easy to produce almost any desired impurity atoms, molecules, or ions.<sup>10–13</sup>

Studies of hydrated ions and ionic water clusters are interesting for a variety of reasons. Many circumstances invariably conspire to make the determination of the detailed structure of bulk hydrogen-bonded systems quite difficult. In liquid systems, in particular, the molecules and atoms are in perpetual motion, due to both thermal excitations and quantum mechanical tunneling. Furthermore, the hydrogen-bonded vibrations are strongly coupled to the low-frequency local motions, contributing to strong homogeneous broadening. Experimentally one usually observes broad, nearly featureless spectral lines due partially to the intrinsic broadening of the states in the condensed phase, partially to extensive spatial and temporal averaging. Most of these effects are substantially reduced in small clusters, which however still provide valuable insights into the structure and properties of the bulk. In particular, ionic clusters are expected to resemble closely the solvation of ions in bulk-phase solutions. Finite clusters are not only easier to study,<sup>14–17</sup> but they are also more amenable to theoretical *ab initio* modeling.

Clusters also provide a convenient medium for studies of aqueous chemistry. As an example, numerous atmospheric processes are believed not to occur really in the gas phase but on droplet and aerosol surfaces, usually aggregates containing a substantial proportion of water. Thus, heterogeneous reactions in the so-called polar stratospheric clouds (PSCs), on the surfaces of micrometer-size particles consisting mainly of inorganic acids and water, are largely responsible for the seasonal ozone depletion, the so-called "ozone hole". Similarly, photochemical smog formation in the troposphere involves surface reactions. One of the major sources of halogens, chlorine and bromine, in the atmosphere is also believed to be the surface oxidation of marine aerosols—effectively small droplets of seawater.<sup>18</sup> Water clusters are obviously surface-rich, and they provide suitable systems for modeling such reactions.

Ionic water clusters are the topic of increasing interest which are intensely studied in many labo-

ratories including our own. Recent studies of ionic water clusters, solvated ions, and their reactions have provided numerous interesting insights and demonstrated that small "nanodroplets" with up to 200 water molecules can also provide a suitable medium for investigating a wide variety of aqueous reactions. The high-resolution Fourier transform ion cyclotron resonance mass spectrometer (FT-ICR MS) has the advantage that the elemental composition of any given cluster can be unambiguously determined, and one can thus examine the reactions occurring in the clusters or on their surface in microscopic, molecular, detail. The purpose of the present paper is to provide a short review of the production, stability, and properties of water clusters. The amount of previous work in this area is truly staggering, and no review of this field can be quite comprehensive. While we have tried to give a fair cross-section of the most important or most recent contributions in the area covered, we put the main emphasis on studies using the FT-ICR technique and, where appropriate, will refer the reader to existing previous reviews dealing with other aspects of ion solvation and water cluster properties. We, however, apologize beforehand for any important studies or contributions which may have been inadvertently omitted.

## II. Experimental Techniques for Cluster Studies

### A. Methods for Generating Water Clusters

In principle, one can imagine two conceptually opposite practical approaches to the problem of generating water clusters. One can either start with a macroscopic solution and disperse it into small droplets whose size can then be further reduced by evaporation or, conversely, begin from the other end, starting with a single atom, molecule, or ion acting as a nucleus, grow under suitable conditions an aggregate with the desired number of water or other ligands around it. Both of these processes occur copiously in nature, and both of them are also extensively used for the production of clusters and droplets in the laboratory.

In nature, clouds in the atmosphere arise from heterogeneous nucleation of supersaturated vapor around suitable nucleation centers, usually preexisting particles or ions. One of the most important laboratory tools in high-energy physics became the cloud chamber developed in 1912 by Wilson. He realized that high-energy particles resulting from radioactive decay ionize gas-phase molecules, which become effective nucleation centers, and droplets formed around them in an environment supersaturated with water vapor will make the particle paths clearly observable. As an example of the natural occurrence of the dispersive process, we have already mentioned that sea spray and dispersion of ocean water result in the formation of marine aerosols.

Also, experimentally there are numerous possible techniques for generating water clusters using both of the above approaches, and a number of them have been described and reviewed in the literature.<sup>10,19–21</sup> The most important of the "dispersive" techniques in the laboratory is undoubtedly the electrospray

method<sup>22–24</sup> employing usually a thin jet of liquid expanding under pressure from a small orifice. Such a thin cylindrical jet will under the effect of surface tension spontaneously break up into small spherical droplets, and these will become electrically charged if a strong electric field is provided in the area of the orifice. If the droplets were expanding into a vacuum, their temperature would quickly drop due to evaporative cooling, they would solidify, and the evaporation would stop. In the electrospray sources, however, the solution expands into a warm gas, so that the temperature of the droplets is maintained and their evaporation proceeds unabated. While the exact details of the ion production mechanisms in the electrospray sources are still controversial, basically the droplets shrink and the charge density on their surface increases until their “fission” or “Coulombic explosion” takes place. This evaporation–explosion sequence process is then repeated until most of the solvent is removed and one gets the charged species of interest.

Perhaps the most important application involves larger organic or biological molecules, which can in this way be gently introduced into the gas phase for mass-spectroscopic studies; but using simple inorganic solutions, it can be used equally well to generate inorganic cations or anions solvated with the remainder of water or other solvents. The organic ions are often multiply charged, for instance, by having many protons attached, but also doubly or even triply ionized metal cations in the gas phase can be generated.<sup>25–27</sup> More detailed information about the technique can be found in several recent books or reviews.<sup>24,28–30</sup>

The dispersive method does not need to depart from liquids, but in principle, one could produce gas-phase ions also by dispersing solid samples. One such technique, extensively applied to hydrated clusters, relies on the sputtering of solid substrates by fast atom or fast ion beams (FAB).<sup>31,32</sup> In a typical experiment, a suitable substrate is bombarded by a rare-gas (Ar, Xe) atom or ion, and accelerated to 1–10 keV. It is perhaps worth noting that the processes occurring when a high-energy atom or ion strikes the sample surface are quite complex, and it is in some cases difficult to assess to what extent the ions and clusters produced represent structures already present in the solid sample and how far they are affected by gas-phase processes occurring during the sample “evaporation”. Experimentally it was, however, for instance, demonstrated that by sputtering ice samples, protonated water clusters  $\text{H}^+(\text{H}_2\text{O})_n$  up to at least  $n = 28$  could be produced and studied.<sup>33</sup> Similarly, by using frozen aqueous solutions or metal samples with an adsorbed layer of ice, one can generate hydrated, or more generally solvated, metal cations, which can then be investigated by secondary-ion mass spectrometry (SIMS), collision-induced dissociation (CID), and other techniques.<sup>34,35</sup>

Conversely, the “aggregating” experimental methods nowadays mostly employ supersonic expansions.<sup>20,21</sup> When a high-pressure gas expands adiabatically into vacuum, the energy of its random thermal motion, as well as the internal vibrational

energy of the gas molecules, their “stagnation enthalpy”, are converted into the kinetic energy of the directed flow and the temperatures in the system sink precipitously. Eventually the gas becomes “supersaturated”, and a spontaneous nucleation can take place. In this way one can, for instance, generate and study even clusters of such weakly bound species such as argon or helium atoms. More often one does not use the expansion of the gaseous substance to be studied alone, but it is entrained or “seeded” into a suitable inert carrier gas, most often helium or argon. In this way, for instance, neutral water clusters can be produced also by expanding a high-pressure inert gas with a small admixture of water vapor. Even more efficient clustering occurs when suitable nucleation centers, such as ions, are provided, for instance, by means of electron impact,<sup>36</sup> electric discharge,<sup>37</sup> or laser vaporization.<sup>38,39</sup>

Studies of hydrated, or more generally solvated, ions in many laboratories very frequently employ such aggregation techniques. Using corona discharge,<sup>40</sup> or even more conveniently laser vaporization,<sup>41,42</sup> ions of the type  $\text{M}^+(\text{H}_2\text{O})_n$  can be generated, where  $\text{M}^+$  may be just about any atomic or molecular ion, e.g.  $\text{H}^+$ ,  $\text{OH}^-$ ,  $\text{Na}^+$ . These ions, produced in an external source, can then be guided and injected into a mass spectrometer for a detailed study. As will be explained later, the water cluster stability and the rates of their fragmentation are limiting the maximum size of clusters which can be investigated in this way. In our existing apparatus, water clusters in the range from 0 to  $\approx 200$  can be studied at the present time.

## B. Techniques for Studies of Ion–Neutral Reactions

There are numerous methods for investigating ion–neutral reactions, with several basic configurations being shown schematically in Figure 1. Each of these experiments proceeds under different conditions and yields slightly different information, with their basic characteristics being listed in Table 1. There are naturally also numerous derivatives, combinations, and modifications of these basic methods. In high-pressure mass spectrometry<sup>43,44</sup> (HPMS) and in experiments where the ion source is coupled to a “fast flow reactor” (FFT) or a “flow tube reactor”,<sup>45,46</sup> the reactions occur at relatively high pressures so that collisions are frequent. The pressure and temperature in such experiments can be well defined, the sample is in thermal equilibrium, and under suitable conditions chemical equilibrium can be reached also.

Such “equilibrium control” work can be exemplified, for instance, by the early studies of ionic water clusters by Kebarle and co-workers<sup>47,48</sup> and by investigations of water cluster reactions with some species of atmospheric interest, such as nitrogen oxides or acetonitrile.<sup>49–51</sup> Also, hydration of  $\text{OH}^-$ ,  $\text{O}_2^-$ , and of the halide anions  $\text{Cl}^-$ ,  $\text{Br}^-$ , and  $\text{I}^-$  was similarly investigated.<sup>52,53</sup> Naturally, in a sample in thermal equilibrium the velocities and energies of the ions are characterized by a Boltzmann distribution and the results averaged over this distribution. From such

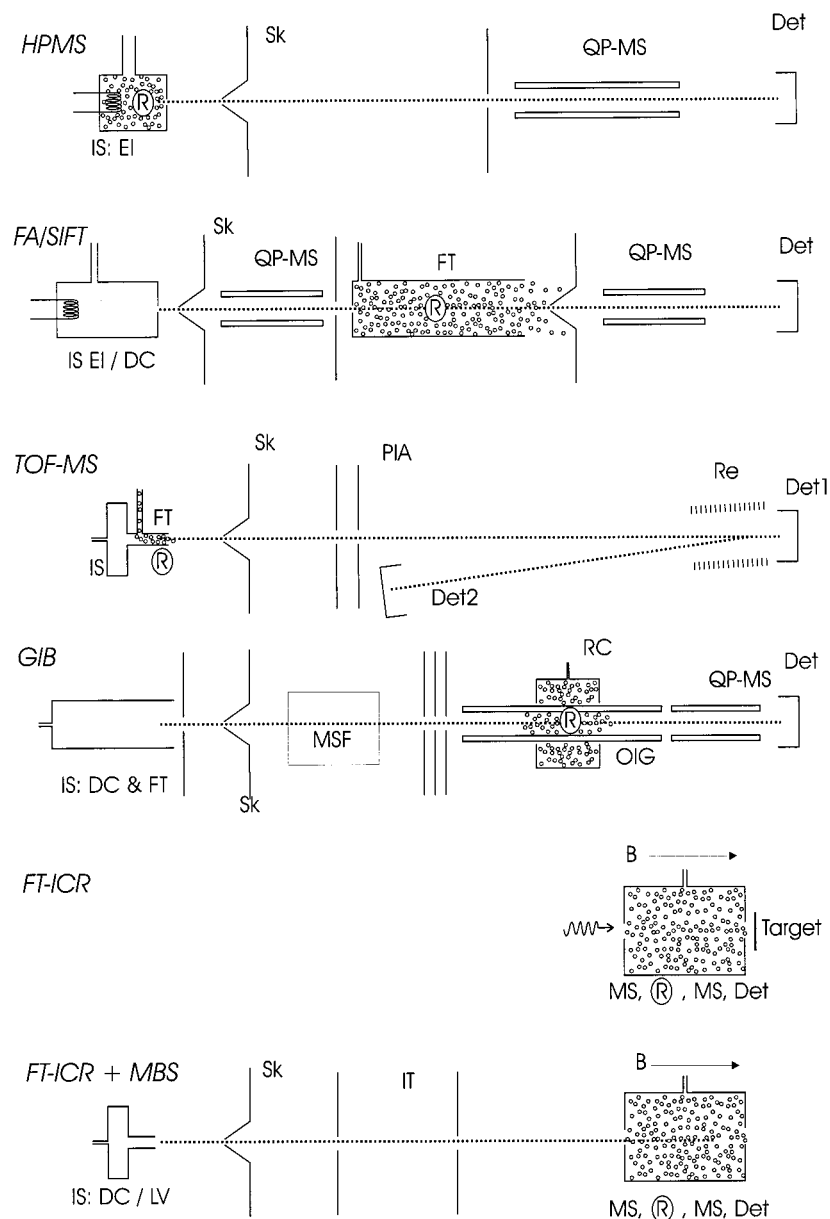


**Figure 1.** Schematic of some basic experimental methods used in ionic cluster studies, as discussed in the text, with some of the typical experimental parameters given in Table 1: (a) HPMS, high-pressure mass spectrometry; (b) FA/SIFT, flowing afterglow/selected-ion flow tube; (c) TOF-MS, time-of-flight mass spectrometry; (d) GIB: guided-ion beam; (e) FT-ICR, Fourier transform ion cyclotron resonance. Some other acronyms and abbreviations: MBS, molecular beam source; IS, ion source; EI, electron impact; Sk, skimmer; DC, discharge; QP-MS, quadrupole mass selection; FT, flow tube; Re, reflectron; Det, detector; MSF, magnetic sector field; OIG, octupole ion guide; RC, reaction cell; B, magnetic field vector; R(encircled), location of reactive encounters; IT, ion transfer; LV, laser vaporization; PIA, pulsed ion acceleration.

**Table 1. Characteristics of Experimental Methods for the Study of Ionic Molecular Clusters**

method	$p$ [mbar]	$t_{\text{coll}}$ [s]	$T_{\text{int}}$ [K]	$E_{\text{kin}}$
HPMS	$\leq 7$	$\geq 2 \times 10^{-8}$	200–500	thermal, $k_b T_{\text{int}}$
FA/SIFT	0.3–0.9	$(1-3) \times 10^{-7}$	130–300	thermal, $k_b T_{\text{int}}$
TOF-MS	$< 10^{-6}$	$> 10^{-2}$	$b$	$\gg 100$ eV
GIB	0.02–0.5 <sup>a</sup>	$5 \times 10^{-6}$ to $2 \times 10^{-7}$	20–300 <sup>b</sup>	thermal to 20 eV
FT-ICR <sup>d</sup>	$< 10^{-7}$	$< 10$	hypertothermal	hypertothermal
FT-ICR+MBS <sup>e</sup>	$10^{-10}$ – $10^{-8}$	1–100	100–180 <sup>c</sup>	$< 1$ eV

<sup>a</sup> Much lower when trapping. <sup>b</sup> Depends on method of cluster generation. <sup>c</sup> Depends on cluster size. <sup>d</sup> When producing small cluster ions in the ICR-cell, e.g., by laser-ablation. <sup>e</sup> MBS: molecular beam source.

experiments one thus derives thermally averaged reaction rates and rate constants and in favorable cases equilibrium constants. A significant number of thermochemical values, such as enthalpies and free

enthalpies of stepwise hydration, have been obtained from such studies.<sup>54</sup> For instance, the first measurements of the binding energies of the hydrated  $\text{H}^+$ - $(\text{H}_2\text{O})_n$ ,  $n = 1, \dots, 8$  ions<sup>55</sup> obtained with the help of



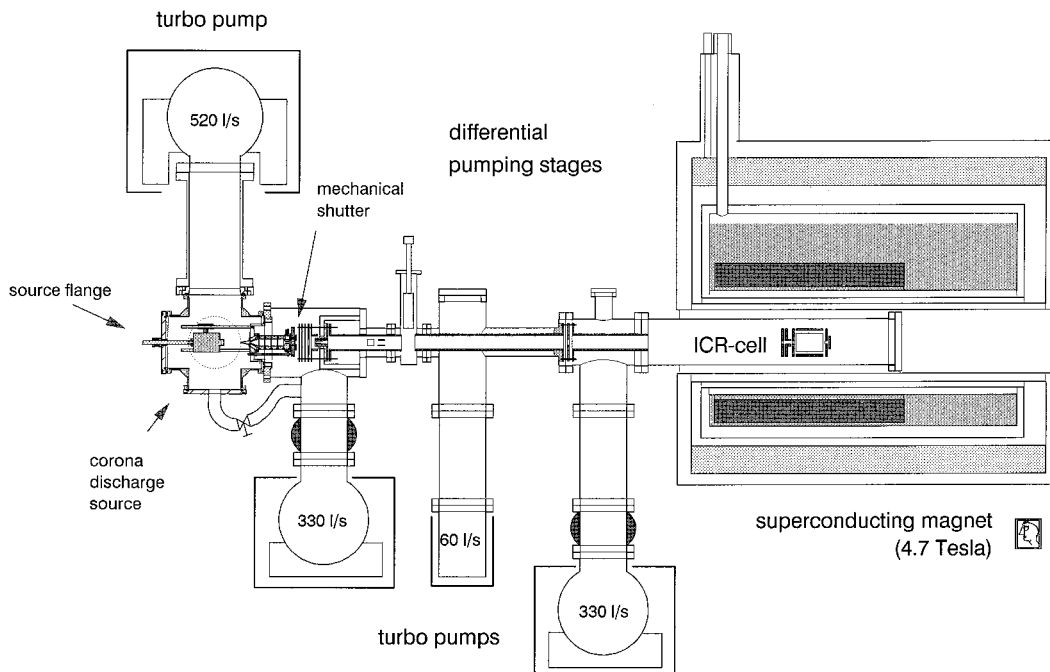


**Figure 2.** Fourier transform ion cyclotron resonance mass spectrometer with an external pulsed supersonic beam ion source. The ions and cluster ions are guided from the source chamber through several stages of differential pumping into the ICR trapping cell. The reactant gases are introduced into the cell via a precision leak valve, raising the pressure from the background value of  $p < 10^{-10}$  mbar to  $\approx 10^{-8}$  mbar, corresponding to about one collision per second.

HPMS yielded values which are very well reproduced by more recent determinations.

Many common ionization methods are nonselective, and the interpretation of the results can be greatly facilitated if one can first mass-select the primary ions, as is done, for instance, in so-called selected-ion flow tube (SIFT) experiments. On the other hand, the injection of ions may require higher, hyperthermal energies, and unless considerable care is taken, the main advantage of the flow tube experiment, a good temperature definition, could be lost. The higher energies can also result in enhanced reactivities and fragmentation and thus complicate the interpretation of the results. The SIFT technique was, for example, used to investigate reactions of the hydrated protons  $\text{H}^+(\text{H}_2\text{O})_n$ ,  $n = 2-11$ , with a variety of gaseous reactants including methanol, ammonia, or acetonitrile.<sup>56</sup> Numerous such studies of water cluster reactions have appeared, and they have also been previously described and reviewed elsewhere.<sup>16,50</sup>

An alternative to SIFT, where the ions may flow through the reaction cell with an essentially thermal energy distribution, is a guided-ion beam experiment (GIB). In this technique pioneered by Teloy and Gerlich,<sup>57</sup> the ions are typically guided through the reaction cell by a high-frequency (RF) octupole field. The technique takes advantage of the fact that ions in a potential field whose direction changes fast compared with the transit time between electrodes experience an effective potential which is relatively flat, except for a sharp rise near the electrodes, preventing ion loss on the cell wall. The advantages of this approach lie in the essential elimination of wall reactions and in an efficient ion collection, resulting in higher accuracy for total cross-section measurements. With the help of a careful control of

the ion beam energy, the binding energies can also be determined in a so-called collision-induced dissociation (CID) experiment, as was, for instance, done for  $\text{H}^+(\text{H}_2\text{O})_n$ ,  $n = 2-6$ , clusters.<sup>58</sup>

In all the above methods, the results and rate constants are averaged over a relatively broad distribution of the reactant kinetic energies. In a better defined "kinetic control" investigation, the velocity and kinetic energy of the reactant ions are known and can be varied and the rate constants determined as a function of the incident ion energy. In such experiments the selected-ion beam of well-defined energy reacts with the desired reactants, but even here, there are a number of possible further refinements and levels of sophistication.<sup>59,60</sup> On the simplest level, the ion beam interacts with a low-pressure neutral gas in a static reaction cell (LPRC). A crossed beam experiment, where the velocity of the neutral reactant is also now isotropic and uniform, represents a further improvement in definition but at the expense of a considerable increase in complexity and a loss in signal intensity. Note that even in this experiment the available energy is not precisely defined, since it will also depend on the impact parameters and geometry. Even more detailed information from such an experiment can be gained by determining not only the total averaged cross-sections but also by detecting the products as a function of the scattering angle.

The technique of choice in our laboratory, Fourier transform-ion-cyclotron-resonance, FT-ICR mass spectroscopy (Figure 2), also has its advantages and disadvantages.<sup>61,62</sup> The ions in the field of a strong, usually superconducting, magnet are confined in a high vacuum ( $10^{-10}$ ) radially by the Lorentz forces resulting in a spiral "cyclotron" motion. The relatively

high, hyperthermal energies of the ions can be a disadvantage of this technique. The maximum kinetic energy can be controlled by adjusting the voltage of the "trapping" electric field confining the ions axially. To keep the ion energy low, we typically use potentials of the order of only 1 V, even though in other laboratories trapping potentials as high as 10 V are common. Since even the 1 eV or  $\approx 8000 \text{ cm}^{-1}$  kinetic energies are considerably higher than the room temperature "thermal" value of  $\approx 200 \text{ cm}^{-1}$ , one may wish to thermalize the ions by admitting a pulse of an inert collision gas, but this can be somewhat cumbersome.

It turns out, however, that even without such a thermalization the higher than thermal energies are often much less of a problem than might appear at first sight. The total kinetic energy of two colliding particles can be written as a sum of two terms,  $\frac{1}{2}MV^2 + \frac{1}{2}\mu v^2$ , where the first term represents the kinetic energy of the center of mass motion in the laboratory coordinates and the latter the energy of the relative motion of the two particles in the center of mass coordinates, where  $v$  is the relative velocity  $|\mathbf{v}_1 + \mathbf{v}_2|$ , and  $M = m_1 + m_2$ . Since the momentum has to be conserved, the first term will remain unchanged by the collision and only the second term is available for nonelastic processes such as exciting one of the partners, fragmentation, or promoting chemical reaction. As long as the reacting ion,  $m_1$ , is much more massive than the collision partner,  $m_2$  (which is often the case in ICR experiments and holds also for large water clusters), then the available energy will be scaled down by roughly the  $m_2/m_1$  ratio and may not deviate very far from typical thermal energies.

### III. Hydrated Ions, their Stability and Structure

In view of the ubiquitous nature of water and the importance of its properties and reactions, both neutral and ionic water clusters have been extensively studied and a comprehensive review would by far exceed the scope of this article. A number of quite "exotic" uses for ionic water clusters have been reported. When, for instance, large clusters are accelerated to high kinetic energies (200 keV) and strike a solid surface, the impact-induced shock results in strong heating. In fact, using deuterated clusters, thermonuclear reactions and formation of tritium within the hot deuterium plasma have initially been reported,<sup>63</sup> but this result has subsequently apparently been retracted.

Of greater interest for the purpose of this review are more chemical applications of water clusters. As already mentioned in the Introduction, a solvent, and most prominently water, stabilizes strongly ions and polar structures and in this way has a profound effect upon the course of chemical reactions. While qualitatively this effect is well-known, quantitative measurements of the stabilization energy of a given ion are difficult, and one circumvents this problem by setting arbitrarily  $\Delta_f H(\text{H}^+, \text{aq}) = \Delta_f G(\text{H}^+, \text{aq}) = 0$  and giving the enthalpies of formation and other thermodynamic functions of all the other ions relative to this standard. This is, in most cases, entirely satisfactory for thermochemical treatment of conventional

reactions of ions or neutrals in solutions, where only the relative ion energies are usually of importance.

Anions or cations never occur in solution alone, but the negative and positive charges are always almost perfectly balanced in bulk solutions, and strictly speaking, the stabilization energy of a given kind of ions will always be a function of all the ions present in the solution and their concentrations. Still, the absolute values of the hydration enthalpies are of interest in cluster ion reactions in the gas phase or in discussing various Born–Haber-type cycles. While direct measurement of an ion hydration energy is difficult, one can, in principle, easily determine the individual sequential, stepwise hydration enthalpies and related properties for the processes of the type  $\text{H}^+(\text{H}_2\text{O})_n + \text{H}_2\text{O} \rightarrow \text{H}^+(\text{H}_2\text{O})_{n+1}$ . Naturally, the limit of such a clustering process around a central ion, for instance  $\text{H}^+$ , is a hydrated proton,  $\text{H}^+(\text{aq})$ . From the hydration enthalpies for different values of  $n$ , the overall hydration enthalpy can, in principle, be evaluated. Whereas the solvent water molecules very close to the central ion are very tightly bound, as one proceeds to higher and higher levels of solvation, the water ligands will eventually be sufficiently remote from the positive charge and the binding energies for the larger and larger values of  $n$  will asymptotically approach the enthalpy of vaporization of water. By adding up the excess binding enthalpies due to the proton for the individual steps and extrapolating to  $n = \infty$ , the absolute values of the overall hydration enthalpy, as well as of the formation enthalpy of the aqueous ion, can be determined.

Such studies of the stepwise hydration enthalpies can conveniently be carried out, for instance, using flow reactors, SIFTs, and related mass-spectroscopic techniques at relatively high pressures where clustering occurs. Thus, in 1967 Kebarle et al. reported the HPMS determination of the proton hydration enthalpies up to  $n = 8$ , and later numerous other experiments of this nature were carried out, with their results extensively reviewed and tabulated.<sup>25,30,54,64–67</sup> When discussing the various techniques available for cluster ion production, we have mentioned already another example of hydration enthalpy determination using a different method. Michl and co-workers were able to produce hydrated protons using FAB bombardment of water ice and determined the stepwise hydration enthalpies up to  $n \approx 28$ .<sup>33</sup>

With the help of the extrapolation of such ion solvation data,<sup>68–71</sup> the absolute values for the thermodynamic properties of an aqueous proton were indeed evaluated and reported, yielding values of  $\Delta_f H(\text{H}^+, \text{aq}) = -1150.1(\pm 0.9) \text{ kJ/mol}$  and  $\Delta_f G(\text{H}^+, \text{aq}) = -1104.5(\pm 0.3) \text{ kJ/mol}$ .<sup>72</sup> These results are in a relatively good agreement with the theoretical value of  $\Delta_f G(\text{H}^+, \text{aq}) = -1118 \text{ kJ/mol}$  derived by extrapolating ab initio computational results,<sup>73</sup> but they deviate from the previously accepted value of  $\Delta_f H(\text{H}^+, \text{aq}) = -1090 \text{ kJ/mol}$ <sup>74</sup> by more than 60 kJ/mol. By similarly extrapolating the water cluster data, one can also attempt to obtain other properties of bulk water otherwise not easily accessible, such as the energy of the conduction band edge and the band gap of bulk water.<sup>75</sup>

An interesting series of studies providing useful insights into the cluster ion stability and the dynamics of their dissociation takes advantage of the fragmentation of metastable species. In numerous investigations of this type, hydrated ions and similar hydrogen-bonded systems were prepared by an electron impact or photoionization of the neutral species in molecular beams. Such ionization usually produces ions with a considerable excess of internal energy, often resulting in their subsequent, delayed dissociation on a microsecond time scale.<sup>76</sup> The ions in most of these studies are then detected in a "reflectron", a type of time-of-flight mass spectrometer, TOF-MS, where the ions are prior to detection reflected by an electrostatic field. The reflectron arrangement was originally designed to compensate for the initial velocity spread of the ions and increase the resolution of the TOF-MS method, but it is also ideally suited for detecting and investigating such a delayed metastable fragmentation. The basic idea of the experiment is that while the parent ions are in the source initially all accelerated to the same velocity, the "daughter ions", produced by delayed fragmentation of the metastable parents and neutral ligand loss, naturally have reduced kinetic energies and are therefore differently affected by the reflecting field and can thus be easily mass-analyzed and identified. In fact, by suitably adjusting the reflecting field, the daughter ions can be completely separated from the parents. The fragmentation pattern as well as the mass peak line shapes of the daughter ions then provide useful insights into the cluster ion structure, stability, and rate of ligand loss, as demonstrated by a series of elegant studies by, e.g., Stace,<sup>77</sup> Castleman,<sup>16</sup> and co-workers.

The solvated electron is another related and quite fascinating topic, which has been the subject of countless studies. Davy has noted already that alkali metals dissolve in ammonia yielding a deep blue solution. It has since been well established that the blue color is caused by strong absorptions of the "solvated electron" in the red and near-IR, and also aqueous electrons are now known to exhibit similar absorptions in this region. It is relatively easy to produce finite "solvated electron" clusters, i.e., water clusters where the "central" ion is simply an electron,  $e^-$ . Clusters of this type can even be produced in a typical laser vaporization source, which is used also in our laboratory, but usually only for larger values of  $n$  above  $\approx 20$ . It is now known that the electron binding energies of small  $(\text{H}_2\text{O})_n^-$  clusters are quite low, but with special care, even  $n = 2$  and all  $n > 5$  clusters could all be detected and investigated. Such hydrated electron clusters are a fascinating subject on their own and have been extensively studied by Johnson and others. Several reviews of this work have also appeared.<sup>19,78-80</sup>

"Pure" water cations, i.e.,  $(\text{H}_2\text{O})_n^+$  clusters carrying a positive charge, represent another interesting topic. Regardless of the method used for ionization of neutral water clusters, such species were usually not detected in any appreciable concentration. Upon closer consideration, this is not so surprising since even though  $\text{H}_2\text{O}^+$  itself is a rather stable ion

isoelectronic with  $\text{NH}_2$ , the ion-neutral reaction  $\text{H}_2\text{O}^+ + \text{H}_2\text{O} \rightarrow \text{H}_3\text{O}^+ + \text{OH}$  is exothermic by almost 2 eV. Apparently all attempts to photoionize neutral water clusters lead to this intracuster reaction and result in their fragmentation and loss of the OH radical, yielding the very stable solvated proton clusters. Ions of this type were also conspicuously absent from the products of the laser vaporization or corona discharge sources. Interestingly, however, the formation of  $(\text{H}_2\text{O})_n^+$  clusters with  $n < 10$  was reported<sup>78</sup> using photoionization of neutral water clusters with an argon atom attached. Here, presumably the departing argon atom may remove excess energy and cool and stabilize the cluster. Since little is known about the internal structure of the clusters produced in this way, it is not clear if this cooling prevents overcoming the activation barrier for the above intracuster ion-neutral reaction or if it simply prevents the OH radical product from evaporating from the protonated water cluster.

In light of the apparent and understandable lack of stability of the  $(\text{H}_2\text{O})_n^+$  clusters discussed above, the recently reported observation of the doubly ionized  $(\text{H}_2\text{O})_n^{2+}$  appears quite puzzling. Stace and co-workers concluded that 100 eV electron impact ionization of neutral water clusters produced besides doubly protonated  $(\text{H}_2\text{O})_n\text{H}_2^{2+}$  clusters also the "pure" doubly ionized species  $(\text{H}_2\text{O})_n^{2+}$ . It should, however, again be noted that nothing is known about the internal structure of these clusters and if they could, for instance, contain two  $\text{H}_3\text{O}^+$  cations and a hydrogen peroxide,  $\text{H}_2\text{O}_2$ , instead of one of the water ligands.

The authors of the above studies have also explored the limits of stability of the doubly ionized ions. The ions in their experiment were accelerated by a 6–8 keV potential and mass-analyzed in a magnetic sector analyzer of their double focusing mass spectrometer. The authors found that the doubly protonated  $(\text{H}_2\text{O})_n\text{H}_2^{2+}$  ions are on the microsecond time scale of their experiment stable only above a certain critical size of about  $n = 35$ . In an interesting further study of the doubly charged ion stability, an ion slightly above this critical size was mass-selected and its fragmentation investigated. When a collision in a CID experiment reduced the number of ligands below this critical  $n = 35$  value, an efficient "fission" or "Coulombic explosion" of the cluster was found to take place. This ion fission was found to be asymmetric, yielding the stable, singly protonated product ions  $(\text{H}_2\text{O})_m\text{H}^+$  with up to about  $m = 26$ . The mass peaks of the fragment clusters produced by the fission are found to be strongly broadened, with the peak widths and profiles providing information about the amount of kinetic energy released in the Coulombic explosion process.

As exemplified above, the interpretation and understanding of many of the experiments are hampered by our lack of knowledge about the internal structure of the cluster species. Structural information about water clusters and similar hydrogen-bonded systems could be obtained by means of optical spectroscopy, but most such studies reported thus far concentrated on neutral species and neutral water



clusters, with the structures of  $(\text{H}_2\text{O})_n$  species being relatively well-known up to about  $n = 10$ .<sup>1,2,4,6,81</sup> High-resolution studies of such neutral water clusters in the far-infrared reveal very complex spectra due to multiple minima potentials and extensive tunneling and proton exchange motions.<sup>4</sup> This is again a fascinating topic which, however, lies largely outside the scope of this manuscript.

FT-ICR mass spectroscopy provides a convenient alternative for investigating ionic water clusters, hydrated ions, and similar hydrogen-bonded systems which, like any other method, has both its advantages and disadvantages.<sup>61,62</sup> When properly applied, it can provide very useful data and information complementary to the reactor or molecular beam work, which was exemplified by a number of interesting representative studies on the preceding pages. The time scale of an FT-ICR experiment is several orders of magnitude longer in comparison with the molecular beam TOF work. Also, in contrast with the ion beams, where the ionization process usually leaves the clusters with an excess internal energy and makes them metastable, the ionic hydrates and clusters produced in an external, supersonic expansion source coupled to an FT-ICR mass spectrometer are initially cold, and by the time the experiment really "starts", they usually have already "survived" several milliseconds. A very useful feature of the method is the superior mass resolution leading to an unambiguous identification of the products. The method has, furthermore, advantages in the easily controlled and well-defined pressure and temperature conditions and in the ability of following the ion reactions and its products for essentially any desired length of time.

The FT-ICR technique can, in principle, also be combined with spectroscopic investigations, as exemplified, for instance, by the trail-blazing studies of Beauchamp<sup>82</sup> and co-workers and by others. In their technique, the ions of interest are "heated" in the ICR cell by absorptions of multiple infrared photons, usually from a  $\text{CO}_2$  laser, leading to their fragmentation, dissociation, electron detachment, or enhanced reactivity. These photoinduced processes are then evidenced by the differences in the mass spectra obtained with the laser on and laser off. By observing the changes in the mass spectra as a function of the laser wavelength, the infrared absorption spectrum of the ion of interest can, in principle, be obtained.

A multiple photon absorption and multiphoton dissociation in a "one color", fixed frequency laser experiment is made possible by the high density of states in larger polyatomic molecules. At higher vibrational energies, the spectra are essentially continuous, so that despite anharmonicity, the absorption of further photons by a "hot" molecule are possible. The line-tunable  $\text{CO}_2$  lasers provide in the infrared a relatively dense (especially if isotopic  $\text{CO}_2$  molecules are used) "picket fence" of discrete lines between  $\approx 800$  and  $1200\text{ cm}^{-1}$ , and in this way, low-resolution spectra of numerous ions could be established. The same technique should obviously also be applicable to ionic water cluster and to hydrated ion

spectroscopy, and several interesting studies in this direction have already appeared and will be discussed later in this review. In fact, our apparatus was originally built with that intent also, but unfortunately we have been thus far unsuccessful in our bids to obtain the necessary funding.

Several thorough reviews discussing various aspects of water clusters have already appeared; both the molecular beam studies and multiphoton fragmentation of the water clusters as well as studies of cluster reactions by HPMS or in flow reactors have been extensively reviewed.<sup>14–17,83</sup> For this reason, the main emphasis in the remainder of the present review will be specifically on the FT-ICR studies of water clusters, but we will discuss the results obtained by other methods wherever necessary for additional insights or comparisons and where appropriate refer the reader to the existing previous works and reviews.

### A. Stability and Fragmentation of Water Clusters

As previously noted, with the help of an external supersonic expansion molecular beam source, clusters of the type  $\text{M}^\pm(\text{H}_2\text{O})_n$  with  $n$  to  $\approx 200$  can be generated and introduced into the ICR cell of the mass spectrometer. The versatile laser vaporization sources can in fact generate not only hydrated ions, but also a wide range of similar solvated species. Thus, the water ligands can be replaced by ammonia,  $\text{HCl}$ , or rare-gas atoms, and the central ions can range from simply an electron or a proton to molecular ions or ionic metal clusters. We have, for instance, investigated clusters of the type  $\text{M}_m^\pm\text{Ar}_n$  where  $\text{M}_m$  is an ionized metal cluster or atom which is solvated by argon atoms. The distribution of the number of ligands depends on the expansion conditions, and in our studies,  $n$  usually ranged 8–10 but if desired could be made much larger. For the purpose of the present paper, we discuss briefly the interesting clear difference observed in the high-vacuum FT-ICR cluster studies in the behavior and stability between the hydrated clusters and the clusters ligated with argon.

The clusters solvated by argon are essentially indefinitely stable in the collision-free environment of the ICR trap.<sup>84,85</sup> On a time scale of many seconds, only very slow reactions are observed, which are due to collisions with the residual gas and result in the gradual loss of the argon ligands or their exchange for water or other residual gas components. The rates of these reactions do not exhibit any pronounced dependence on the cluster size, i.e., on the values of  $m$  and  $n$ . Unlike the clusters solvated by argon, the water clusters steadily fragment on a much faster, millisecond time scale, even though the water ligands are surely much more strongly bound.<sup>86</sup> Regardless of the initial size distribution, after a sufficiently long time, typically about 60 s, only one unique product cluster  $n = 4$ , i.e.,  $\text{H}^+(\text{H}_2\text{O})_4$ , remains. Experiments with size-selected clusters show that the ligands are lost one by one at a steady pace, and furthermore, one finds out that the rate of fragmentation is in this case not cluster size independent but to a fairly good approximation linearly proportional to the number



of ligands  $n$ . In this regard it should perhaps still be noted that in investigations with other ligands, clusters solvated with other rare gases or molecular oxygen,  $O_2$ , are found to behave in this respect similarly to the argon cluster<sup>87</sup> while clusters solvated with ammonia,  $M^{\pm}(\text{NH}_3)_n$  ( $n = 1-100$ ), parallel almost exactly the behavior of the hydrated ions.<sup>88</sup>

The steady fragmentation of the water and ammonia clusters implies that even in the collision-free high-vacuum environment there is a steady energy input. The difference between the rare gases, Ar or Xe, or  $O_2$ , on one hand, and the water or ammonia ligands, on the other, is that only the latter can efficiently absorb infrared light. While neither of the former ligands absorbs in the infrared, both  $H_2O$  and  $NH_3$  have a strong IR vibrational spectrum, which is strongly enhanced both by hydrogen bonding between the ligand molecules and by their strong binding to the central ion. The observed consecutive loss of ligands is due to the absorption of the infrared blackbody radiation from the apparatus walls. This effect was first observed and correctly diagnosed for several small ionized water clusters by McMahon and co-workers.<sup>89,90</sup> In our laboratory the fragmentation studies were extended to large water clusters and the mechanism confirmed both by varying the wall temperature and by experiments with deuterated clusters.<sup>11,41,86</sup>

## B. Infrared-Induced Fragmentation

As an interesting historical aside it is perhaps appropriate to mention that the idea of blackbody-driven chemical reactions and fragmentation is not at all new. Nearly 100 years ago an, at that time puzzling, observation was made that a number of reactions believed to be activated by collisions exhibited first-order pressure dependence. The French physicist Perrin suggested that these reactions might actually be activated by infrared radiation,<sup>91</sup> but the idea was promptly dismissed and disproved by others.<sup>92</sup> The mystery was solved by Lindemann with his theory of collisional activation of unimolecular reactions,<sup>93</sup> which was later extended and refined by Hinshelwood.<sup>94</sup>

The gist of the theory, which can today be found in any introductory book on physical chemistry, is that the product formation proceeds via an activated complex  $A^*$  and is characterized by a competition between its spontaneous decay into products and collisional deactivation back to the reactant A. While at low pressures the collisional deactivation is negligible and the product formation is a quadratic function of pressure, at higher pressures a dynamic equilibrium between A and  $A^*$  is established. In other words, the lifetime of activated  $A^*$  becomes inversely proportional to pressure with the product formation being only a linear function of  $p$ . If one writes for the product formation an equation in the form of  $d[P]/dt = k_{\text{ef}}[A]$ , then the "effective rate constant" will really appear constant at high pressures where the rate of  $A^*$  collisional deactivation is faster than the rate of its spontaneous decay but below this pressure this rate "constant" will become proportional to pressure, with the rate extrapolating to zero at zero pressure.

It is quite trivial to extend this model to include the possibilities of activation or deactivation by emission or absorption of light by simply including, besides the collisional rate constants  $k^+$  and  $k^-$ , two additional rate constants,  $k^{\text{abs}}$  and  $k^{\text{em}}$ . Making the usual assumption of a steady-state-activated complex concentration, one gets

$$\frac{d[A^*]}{dt} = k^+[A^2] + k^{\text{abs}}[A] - k^-[A^*][A] - k^{\text{em}}[A^*] - k^*[A] = 0$$

$$\frac{d[P]}{dt} = k^*[A^*] = \frac{k^*(k^+[A^2] + k^{\text{abs}}[A])}{k^* + k^{\text{em}} + k^-[A]} \approx \frac{k^*k^{\text{abs}}[A]}{k^* + k^{\text{em}}}$$

When the pressure becomes so low that the collisional processes can be neglected, one gets a product formation rate proportional to the reactant concentration, i.e., a pressure-independent first-order decay constant  $k^{\text{ef}} = k^*k^{\text{abs}}/(k^* + k^{\text{em}})$ . The  $k^{\text{abs}}$  and  $k^{\text{em}}$  used in this expression are not really constants but depend on a number of factors. Without going into details, one can first remember that the integrated intensity of blackbody emission is roughly proportional to  $T^4$  and that at ambient temperatures it will be very low with a maximum in the far-infrared near  $600 \text{ cm}^{-1}$ . In the second place, the infrared fluorescence lifetimes are very long, typically on the order of many milliseconds to seconds, the corresponding absorptions weak, and the rates of photon absorption low. As a result, one can only hope to observe the effects of the blackbody radiative heating if the rates of collisional processes can be brought into a sufficiently low range and the reactants A can be observed for a sufficiently long time. This is only the case in the ultrahigh vacuum of an ion trap, e.g., in an FT-ICR mass spectrometer or in low-temperature matrices,<sup>95-97</sup> and this is also the reason that such processes have become observable and amenable to experimental study only fairly recently.

The fragmentation of size-selected clusters ranging from  $n = 1$  to above  $n \approx 100$  has now been explored in detail with some of the results reproduced in Figures 3 and 4. One can clearly note that neglecting clusters  $n \leq 4$ , which on the time scale of the experiment do not fragment at all, the rates are proportional to the size of the cluster  $n$ , or more exactly they can be well fitted to a linear equation  $r_n = k(n - n_0)$ , where  $n_0$  is the abscissa intercept and  $k$  is the slope. The water vapor in the supersonic expansion source is highly diluted, and the clusters are initially produced cold. Each time a water molecule evaporates it removes from the cluster an amount of heat comparable to its binding energy, roughly the sublimation energy of water. By taking into consideration the heat capacity of the clusters, one can deduce that the temperature of clusters around  $n = 50$  will be lowered by about 10 K each time one water ligand evaporates, which in turn should lower the rate of further evaporation by about a factor of 20 in the collision-free environment.<sup>86</sup> Despite that, one finds that the evaporation proceeds at a steady pace, with a molecule of water being lost about every 100 ms. It is fairly clear that after water ligand is lost an

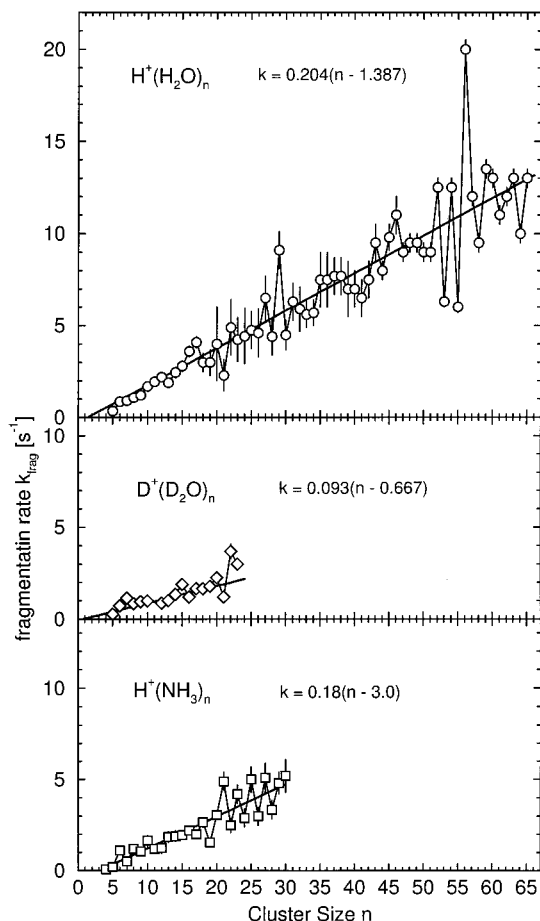


**Figure 3.** Rates of the blackbody radiation-induced fragmentation of solvated cation clusters as a function of the number of ligands showing the overall linear dependence discussed in the text. The rate of energy absorption, and thus also the rate of fragmentation, is roughly proportional to the number of ligands  $n$  but note the deviations, e.g., for the  $n = 21$  and  $55$  “magic” clusters. The distinctly steeper slope of the  $\text{H}^+(\text{H}_2\text{O})_n$  plot in the top trace compared with the deuterated  $\text{D}^+(\text{D}_2\text{O})_n$  data in the middle panel is due to isotopic changes in the infrared spectrum and reduced overlap with the 300 K Planck blackbody curve for the heavier isotope. The bottom trace shows that also ions solvated by ammonia,  $\text{NH}_4^+(\text{NH}_3)_n$ , exhibit similarly efficient fragmentation. The fact that also the slope and the proportionality constant is similar to that of water clusters is basically fortuitous.

energy approximately equivalent to its binding energy has to be absorbed before another ligand can evaporate. The rate of the absorption is proportional to the overlap integral between the blackbody radiation density function  $\rho(\lambda, T_w)$  at the temperature of the apparatus walls  $T_w$  with the infrared absorption spectrum of a given  $\text{H}^+(\text{H}_2\text{O})_n$  cluster,  $\sigma_n(\lambda)$

$$k_n^{\text{abs}} = k \int_0^\infty \sigma_n(\lambda) \rho(\lambda, T_w) d\lambda \approx k'n$$

Since the ligands, in the present case the water molecules, are the absorbers, both the integral of the absorption intensity  $\sigma_n(\lambda)$  and the value of its overlap integral with the Planck function  $\rho_n(\lambda)$  should be approximately proportional to the number of water ligands  $n$ . Consequently, the overall energy absorption rate as well as the rate of evaporation should be

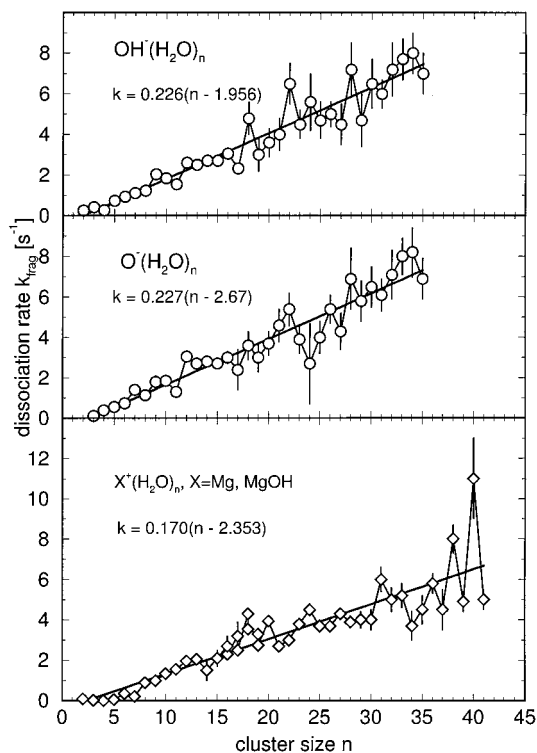


**Figure 4.** Blackbody radiation-induced fragmentation rates of various size-selected hydrated ions. The experimental points are given by the open symbols with statistical error bars; the solid lines represent linear fits of the data. Note that the slopes for different central ions are similar; the slight differences fit parameters summarized in Table 2 and are more dependent on the different data field used than on the specific nature of the central ion.

proportional to  $n$ , consistent with the experimental observation.

The initial temperature of the clusters emerging from the source should be around 40 K based on the expansion conditions, but once in the collision-free environment, it will be controlled by the competition between their radiative heating and evaporative cooling. The temperatures will be size dependent, and from the rate of evaporation and bulk properties of water, one can crudely assess that clusters around  $n = 50$  will have temperatures of about 120 K. At this temperature, the rate of the “blackbody” emission from the clusters will be more than an order of magnitude smaller than the rate of absorption of the blackbody radiation from the apparatus walls and can be neglected. As one proceeds to smaller and smaller clusters, the water ligands get closer and closer to the positive charge and become more and more strongly bound. The temperature of the smaller clusters thus has to rise higher before their evaporation can proceed. Eventually the smallest clusters will reach the temperature of the ambient walls, at which point they will be in thermal equilibrium with their environment, the rate of absorption by the clusters will be identical to the rate of their emission, and the heating process will stop.

This is undoubtedly the case for the  $n = 4$  and smaller clusters, for which no further fragmentation is observed. The lack of further ligand loss simply reflects the fact that the binding energies are too high

and the rate of fragmentation at room temperature is negligibly small on the time scale of our experiment (up to  $\approx 1$ –3 min). The fact that very small clusters do not further fragment is also the physical reason for the abscissa intercept of the linear fits and for the need for the  $n_0$  constant in fitting the data to be discussed below. At the opposite end of the size scale, the fast fragmentation of large clusters explains why meaningful studies of cluster reactions in our apparatus are restricted to about  $n = 200$ . Obviously the evaporation rates could be reduced and larger clusters studied with an apparatus with a variable wall temperature, and further work in this direction is currently in progress.

For small values of  $n$ , the infrared spectra of the clusters can be fairly easily computed by the DFT techniques. While the accuracy of the absolute values of the absorption intensities and of the overlap integrals are difficult to assess, the computed relative rates  $k_n^{\text{abs}}$  permit further convenient checks of the above model. Such calculations, for instance, predict approximately a factor of 2 smaller overlap integrals for fully deuterated clusters, in excellent agreement with the experimental finding that the  $\text{D}^+(\text{D}_2\text{O})_n$  clusters fragment approximately a factor of 2 more slowly<sup>86</sup> than the corresponding normal water clusters. Similarly, consistent with the model prediction, it is found that increasing the wall temperature to about 370 K increases the fragmentation rate by about a factor of 2.5.

Theoretical modeling of the infrared absorption spectra allows another interesting observation. They, for instance, reveal that even though the OH and OD stretching vibrations are by far the strongest infrared bands in the spectrum, they are too far removed from the maximum of the 300 K Planck curve to contribute substantially to the cluster heating. Major contributors to the blackbody absorption are the weaker, lower-frequency deformation modes, essentially due to hindered rotational and translational motions of the water molecules. In contrast with water or ammonia clusters, for systems where hydrogen bonding is of lesser importance, an increase in the fragmentation rates was reported upon deuteration of hydrocarbons.<sup>98</sup> This may reflect the improved overlap of the lower CD bending and stretching vibrations of the deuterated compounds with the blackbody radiation and suggest that the low-frequency deformations are in this case too weak to make the dominant contribution to the IR absorption.

### C. "Magic" Cluster Sizes

Even though, as discussed above, the cluster fragmentation rate is to a fair approximation proportional to the number of ligands  $n$ , examination of Figures 3 and 4 immediately reveals that some particular sizes deviate from this dependence by amounts far outside the measurement accuracy. One of these "magic" values,  $n = 4$ , has already been discussed above. The water molecule has an extremely high proton affinity and forms a very stable  $C_{3v}$  symmetry  $\text{H}_3\text{O}^+$  hydronium ion with three equivalent protons. Each of these carries a considerable positive charge

and can again strongly bind an oxygen atom of an additional water ligand. In this way,  $n = 4$  essentially completes the first solvation layer, as already concluded by Eigen.<sup>99,100</sup> The fifth and all additional ligands are already bound much more weakly, and as shown in Figure 3, all the  $n > 4$  clusters exhibit observable fragmentation rates.

A further cluster exhibiting a consistently anomalous behavior is  $n = 21$ , as reported already more than 25 years ago by Fenn and co-workers,<sup>10</sup> who observed its enhanced abundance, which they interpreted in terms of a particularly stable dodecahedral clathrate structure of 20 water ligands around a central hydronium ion. The enhanced stability of the  $n = 21$ , presumably  $\text{H}_3\text{O}^+(\text{H}_2\text{O})_{20}$  cluster, has been confirmed in a large number of later experiments. Regardless of whether the neutral water clusters were ionized by electron impact or by vacuum UV, whether produced in supersonic expansions, in a flow reactor, or in secondary-ion mass spectra of a solid ice surface, an anomalous abundance of the  $n = 21$  cluster was always detected.<sup>32,101–109</sup> Finally, reactions of the preformed protonated water clusters have shown that the  $n = 21$  species can bind up to 10 dimethylamine molecules, presumably attached to the 10 dangling OH bonds, consistent with the proposed dodecahedral structure.<sup>110,111</sup> Less convincing evidence was reported for a special stability of a shell of 20 water molecules around other central ions, for instance  $\text{OH}^-$ ,<sup>112,113</sup>  $\text{Cs}^+$ ,<sup>114</sup> and other alkali cations.<sup>115</sup> Also, authors of a later reinvestigation of this type of complexes which included molecular dynamics simulations were in support of the clathrate interpretation.<sup>116</sup>

The ICR experiments, even though confirming unambiguously the anomalous behavior and enhanced stability of the  $n = 21$  cluster, do not give any information about its structure. Our lifetime measurements on size-selected ions show that the  $n = 21$  cluster fragments nearly a factor of 2 more slowly than  $n = 20$  and even more significantly reveal that the  $n = 22$  cluster, with one additional molecule outside the stable shell, fragments particularly efficiently, more than a factor of 3 faster than  $n = 21$ . While the enhanced stability is beyond doubt, the evidence for the "clathrate" dodecahedral structure, on the other hand, appears much less convincing. Water is, of course, well-known to form under high-pressure clathrate solids with cage-like cavities, which often possess dodecahedral structures and contain molecular or atomic inclusions or "guests".<sup>117–119</sup> In nature, there are in fact enormous reserves of such clathrates containing methane in the permafrost and in deep oceans, which may represent a largely untapped source of energy, and similar solid hydrates with trapped molecular  $\text{CO}_2$  have recently been considered as a possible means for disposing of carbon dioxide, the gas mainly responsible for the "greenhouse effect", deep in the oceans.

The guests in these clathrates are, however, invariably hydrophobic species with isotropic or nearly isotropic potentials such as methane or rare gases, Ar, Kr, or Xe, while as mentioned above, the potential of the hydronium ion,  $\text{H}_3\text{O}^+$ , is highly anisotropic and



directional and clearly prefers to bind strongly and specifically to three and only three water ligands. How the binding of the  $\text{H}_3\text{O}^+$  cation would be realized in a dodecahedral shell is not at all obvious. In any event, if such a closed shell of 20 water molecules around the hydronium cation indeed forms, it will very likely be strongly distorted from a dodecahedral structure. Recent theoretical studies combining molecular dynamics with computed ab initio potentials and forces have found for  $\text{H}_3\text{O}^+(\text{H}_2\text{O})_{20}$  a distorted dodecahedral structure, however, with several other compact structures at essentially the same energy and with all of them exhibiting 10 dangling OH bonds.<sup>120</sup>

Interestingly, recent FT-ICR work, extending the hydrated proton fragmentation studies to much larger clusters, has clearly revealed a similar anomaly for the  $n = 55$  cluster, which is almost as clear and prominent as that of the  $n = 21$  structure. The anomalous behavior could be confirmed by at least three different independent means.<sup>121</sup> The  $\text{H}^+(\text{H}_2\text{O})_{55}$  cluster is under a wide range of conditions consistently much more abundant than its neighbors. When the fragmentation of size-selected ions is investigated, one finds that the  $n = 55$  cluster fragments more than a factor of 2 more slowly than  $n = 54$  and again the  $n = 56$  shows anomalously low stability and fragments more than a factor of 3 faster than  $n = 55$ . Finally, if one selects one of the larger clusters, e.g.,  $n = 58$  or  $n = 60$ , and follows its sequential fragmentation process, one observes that the  $n = 55$  "sticks around" much longer than its neighbors,  $n = 54$  or  $56$ , with time-integrated intensities of the  $n = 56, 55$ , and  $54$  fragment ions again being consistent with the above-mentioned ratio of their individual decay rates. Any proposal of a concrete structure of the  $\text{H}^+(\text{H}_2\text{O})_{55}$  ion would naturally be even more speculative than that of the  $n = 21$  species. It is, however, interesting that one can again construct reasonable structures with pentagonal symmetry.

Interesting in this connection are recent observations of Beauchamp and co-workers.<sup>122</sup> Their FT-ICR study confirmed the special abundance of the  $n = 21$  and  $55$  solvated proton clusters but also found that inclusion of a singly protonated primary amine into the cluster shifted the "magic" numbers of the water ligands to  $n = 20$  and  $54$ , respectively. This would suggest that in these clusters a protonated amino group of the  $\text{R}-\text{NH}_3^+$  species replaces the hydroxonium  $\text{H}_3\text{O}^+$  ion in the solvated proton clusters, which in turn would seem to imply that the  $\text{H}_3\text{O}^+$  ion is an integral part of the cage rather than being located centrally within it.

There is, however, perhaps one interesting conclusion that can be drawn from the so prominently enhanced stabilities of the  $n = 21$  and  $55$  ions. An important question one may ask is whether the hydrated clusters should instead be regarded as solids or as liquids, i.e., whether they have well-defined equilibrium structures or should they better be viewed as a more or less random mixture of numerous isomers. If the latter was true, one might expect that the deviations in behavior would average out and that one would observe a much smoother

dependence of properties on  $n$ . The large deviations of some clusters from linear dependence would strongly suggest that they cannot be viewed as floppy liquid droplets but that even clusters as large as  $n = 55$  must possess well-defined structures.

#### D. Effect of the Central Ion

While in the discussion above we have focused our attention on the hydrated proton clusters, stability and blackbody fragmentation have been investigated for numerous other hydrated ions. When pure water clusters are investigated, the cations formed are almost exclusively of the solvated proton variety and as already discussed pure  $(\text{H}_2\text{O})_n^+$  ions are not detected. Extraction of anions employing a corona discharge ionization source, on the other hand, results in a much larger variety of  $\text{X}^-(\text{H}_2\text{O})_n$  ions. While the aggregates with central hydroxyl anion ( $\text{X} = \text{OH}$ ) under most conditions prevail, ions with  $\text{X} = \text{O}, \text{O}_2$ , and  $\text{O}_2\text{H}$  are also present, and under certain conditions even solvated electrons ( $\text{X} = \text{e}$ ) are produced.<sup>41,123</sup>

Using the laser vaporization source, a variety of clusters with the central ion involving essentially any desired element can be prepared. For instance, hydrated cation clusters where the central ion was  $\text{Mg}^+, \text{Ca}^+$ , or  $\text{Al}^+$ , or chlorides or hydroxides of these metals,  $\text{MgOH}, \text{MgCl}, \text{Al}(\text{OH})_2$ , or  $\text{AlCl}_2$ ,<sup>37,112</sup> were all rather extensively investigated,<sup>42,124</sup> as well as both cations and anions of iodine, i.e., hydrated  $\text{I}^+$  and  $\text{I}^-$ .<sup>125,126</sup> In each of these cases an ion of any given value of  $n$  can be mass-selected and its fragmentation rate studied and fitted as described for the hydrated protons. Independent of the specific nature of the central ion, one always observes the approximately linear relationship between the fragmentation rate and the number of ligands  $n$  and can obtain from the fit of the data the abscissa intercept  $n_0$  and the proportionality constant  $k$ . The constants obtained in this way for a variety of anions and cations are listed in Table 2.

Two general observations can be made from these data. In the first place, examination of the data, for instance, in Figures 3 and 4 reveals that while in most cases one can find specific cluster sizes whose stability and fragmentation rates deviate from the general linear size dependence, the "magic" numbers are in general different for different central ions. The central ion, therefore, apparently has some influence on the preferred structure of the hydrated cluster, and this influence affects not only the first and second solvation shells but seems to persist up to fairly large clusters—note for instance that the anomalous behavior of solvated proton with  $n = 21$  or  $55$  discussed above is not observed with other central ions.

A second conclusion one can make either by examining Figures 3 and 4 or comparing the constants derived from the separate data in Table 2 is that the values of the proportionality constant  $k$  between the number of ligands  $n$  and the rate of water ligand loss do not depend strongly on the specific nature of the central ion. The constants are very nearly the same, regardless of whether it is a cation or anion and

**Table 2. Experimental Studies on the Blackbody Radiation-Induced Fragmentation of Ionic Water Clusters and Related Compounds**

cluster	cluster size range $n^a$	temperature range [K]	rates of H <sub>2</sub> O loss (s <sup>-1</sup> ) and other determined quantities	ref
H <sup>+</sup> (H <sub>2</sub> O) <sub><i>n</i></sub> <sup>a</sup>	2–4	295–309	$k(p, T)$ , $\Delta H_{298}^\circ$ , $\Delta G_{298}^\circ$ , $\Delta S_{298}^\circ$	89
Cl <sup>-</sup> (H <sub>2</sub> O) <sub><i>n</i></sub>	2–4	295–309	$k(p, T)$ , $\Delta H_{298}^\circ$ , $\Delta G_{298}^\circ$ , $\Delta S_{298}^\circ$	89, 90
Cl <sup>-</sup> ((CX <sub>3</sub> ) <sub>2</sub> CO) <sub><i>n</i></sub>	1	303	$k(p, T)$	98
Cl <sup>-</sup> (C <sub>6</sub> X <sub>6</sub> ) <sub><i>n</i></sub>	1	303		
X <sub>3</sub> O <sup>+</sup> ((CX <sub>3</sub> ) <sub>2</sub> O) <sub><i>n</i></sub> , X = H, D	2, 3	303		
H <sup>+</sup> (H <sub>2</sub> O) <sub><i>n</i></sub>	5–65	298–340	$k = 0.204(n - 1.387)^a$	86, 121
D <sup>+</sup> (H <sub>2</sub> O) <sub><i>n</i></sub>	5–35	298	$k = 0.093(n - 0.667)$	
OH <sup>-</sup> (H <sub>2</sub> O) <sub><i>n</i></sub>	2–35	298	$k = 0.226(n - 1.956)$	41
O <sup>-</sup> (H <sub>2</sub> O) <sub><i>n</i></sub>	3–35		$k = 0.227(n - 2.670)$	121
e <sup>-</sup> (H <sub>2</sub> O) <sub><i>n</i></sub>	21–27		$k = 0.207(n + 0.623)$	
Mg <sup>+</sup> (H <sub>2</sub> O) <sub><i>n</i></sub>	2,3,16–41	298	$k = 0.170(n - 2.353)$	41
Mg(OH) <sup>+</sup> (H <sub>2</sub> O) <sub><i>n</i></sub>	4–19			42
Al <sup>+</sup> (H <sub>2</sub> O) <sub><i>n</i></sub>	4–45	298	$k = 0.16(n - 1.63)$	11
Al(OH) <sub>2</sub> <sup>+</sup> (H <sub>2</sub> O) <sub><i>n</i></sub>	11–24			124
I <sup>-</sup> (H <sub>2</sub> O) <sub><i>n</i></sub>	1–12	298	$k = 0.17(n - 1.53)$	126
I <sup>+</sup> (H <sub>2</sub> O) <sub><i>n</i></sub>	1–15	298	$k = 0.17(n - 3.41)$	125
(G + 2H) <sup>2+</sup> (H <sub>2</sub> O) <sub><i>n</i></sub> , G = Gramicidin	0–50	298–509	$16 \leq k(298 \text{ K}) \leq 230$	13, 174
Ca <sup>2+</sup> (H <sub>2</sub> O) <sub><i>n</i></sub>	5–7	293–483	$k(T)$ , $E_a$ , $E_0$ , $\Delta H_{298}$	26
Ni <sup>2+</sup> (H <sub>2</sub> O) <sub><i>n</i></sub>	6–8			
H <sub>3</sub> O <sup>+</sup> (H <sub>2</sub> O) <sub><i>n</i></sub>	2–3			
Mg <sup>2+</sup> (H <sub>2</sub> O) <sub><i>n</i></sub>	6666	293–413	$k(T)$ , $E_a$ , $E_0$ , $\Delta E_{\text{binding}}$	27
Ca <sup>2+</sup> (H <sub>2</sub> O) <sub><i>n</i></sub>				
Sr <sup>2+</sup> (H <sub>2</sub> O) <sub><i>n</i></sub>				
Ba <sup>2+</sup> (H <sub>2</sub> O) <sub><i>n</i></sub>				
C <sub>6</sub> H <sub>5</sub> COCH <sub>3</sub> <sup>+</sup>		1100–1600	$k(T)$ , $E_0$ , $\Delta E$ , $\Delta H_{298}^\circ$	175,176
C <sub>6</sub> D <sub>5</sub> COCD <sub>3</sub> <sup>+</sup>				

<sup>a</sup>  $n$  is the cluster size, equal to the number of water molecules attached.

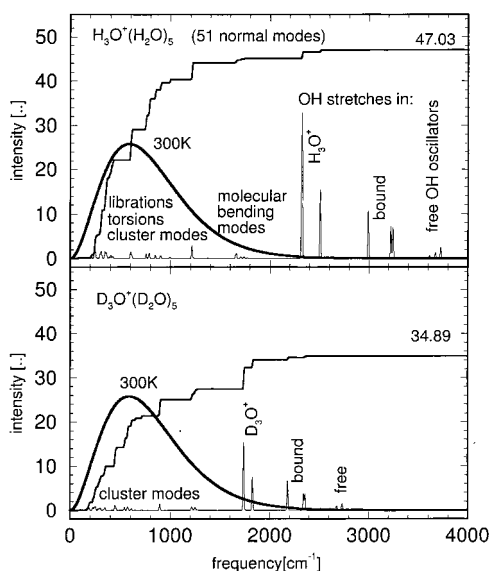


**Figure 5.** Convolution of the 300 K blackbody radiation curve with the calculated absorption spectra of H<sup>+</sup>(H<sub>2</sub>O)<sub>6</sub> (top) and D<sup>+</sup>(D<sub>2</sub>O)<sub>6</sub> (bottom). The spectra computed by DFT techniques for optimized cluster structures<sup>172</sup> indicate that mainly the low-frequency “cluster” translational or librational deformation modes, rather than the OH bending and stretching vibrations, contribute to the energy absorption. Note that in agreement with the slopes in Figure 2, the overlap integral for the deuterated clusters is significantly smaller than that of normal water clusters.<sup>121</sup>

whether it is monatomic or molecular. The slight variations found in the table, ranging from about 0.16 to 0.22, are more the result of the various data fields of the fits—the exact range of cluster sizes produced varies somewhat from experiment to experiment—than of real differences due to the central ion. The

major exception is the result with the deuterated clusters, for which the slope  $k$  is found to be a little more than a factor of 2 smaller than for normal water. The major contribution to this effect naturally lies, as discussed above, in the isotopic shifts in the vibrational spectrum and its resulting reduced overlap with the 300 K blackbody curve (cf. Figure 5). There may also be minor contributions due to zero-point energies and similar effects.

The observation that the constant  $k$  is insensitive to the specific nature of the ion is probably reasonable, for in a sufficiently large cluster the molecules at its periphery will feel the screened potential of the central ion only weakly and their evaporation will resemble the evaporation of pure water. Note, however, that there may be some contradiction in this statement with the argument in one of the preceding paragraphs that the central ion seems to influence the overall structure of the hydrated cluster up to rather large values of  $n$ .

## E. Ions in Pure Water and the Structure of the Aqueous Proton

From our terrestrial point of view, with nearly  $3/4$  of the earth’s surface being covered by oceans, water is surely the most important solvent which possesses a large number of interesting properties. One of its key properties as a solvent is the high polarity of water molecules and the resulting ability to stabilize ions and ionic structures. This can be easily demonstrated by examining the pure water itself and considering the simple fact that it is even at room temperature partially ionized. To generate the H<sup>+</sup> and OH<sup>-</sup> ions from gas-phase H<sub>2</sub>O molecules, 1627.74 kJ/mol would have to be expended. The polar water

molecule has, however, a very high proton affinity, so that a single additional "solvent" molecule reduces the enthalpy of the ionization reaction by nearly one-half



Even so, if one calculated how many molecules would at room temperature be ionized by this gas-phase reaction, one finds out that it is less than 1 in  $10^{160}$ , a number exceeding by many orders of magnitude the number of atoms in the universe. Actually we know, however, that in 1 L of pure water there will at room temperature be  $10^{17}$  protons with a corresponding number of  $\text{OH}^-$  anions. This number would correspond to reducing the enthalpy of the above reaction from 933 to 22 kJ/mol. This reduction is due to a further solvation of the  $\text{H}_3\text{O}^+$  and  $\text{OH}^-$  ions. The presence of these ions, the ability to change their relative concentrations, and their high mobility contribute greatly to the important properties of water as a solvent in the industry, in nature, and in the chemistry of life.

The ability of an ICR experiment to produce discrete clusters containing  $\text{H}_3\text{O}^+$  or  $\text{OH}^-$  ions permits investigations of their stability, fragmentation, and chemistry, which in turn may provide some additional insights into topics such as ion solvation, charge and proton transfer, and proton mobility. As noted above, the description of the positive charges in solution as either "protons" or as  $\text{H}_3\text{O}^+$  is not quite accurate, since the ion is further solvated, and the same holds for the hydroxyl anions. The actual form of the ions present and their solvation geometry were the subject of extensive experimental and theoretical studies.

The proton is unique among all cations in that it has no electrons and, therefore, from a chemical point of view no dimensions. In a recent investigation of a proton solvated by rare-gas atoms, it could be shown using a very simple electrostatic model that the proton will always be solvated by two and only two ligands in a linear symmetric arrangement in the first solvation shell. While the study involved specifically rare-gas atoms, there is little doubt that the same simple model should hold for simple molecular ligands as well and would, therefore, predict rather stable hydrated  $\text{H}_2\text{O}\cdots\text{H}^+\cdots\text{OH}_2$  entities. The importance of such ions for aqueous ions was, in fact, suggested by Zundel quite some time ago<sup>127</sup> and are sometimes associated with his name. Their properties have been extensively studied both theoretically and by experiment, with both finding in an essential agreement a centrosymmetric, linear bond in an ion close to  $D_{2h}$  symmetry. While strictly speaking the computations yield a potential with degenerate stationary points of  $C_2$  symmetry, the energy of the transition state for their interconversion is only  $\approx 1.5$  kJ/mol, considerably lower than the zero-point energy.<sup>128</sup>

The situation in larger systems and in the liquid phase is, however, not necessarily so simple. As noted above, water has an extremely high proton affinity,

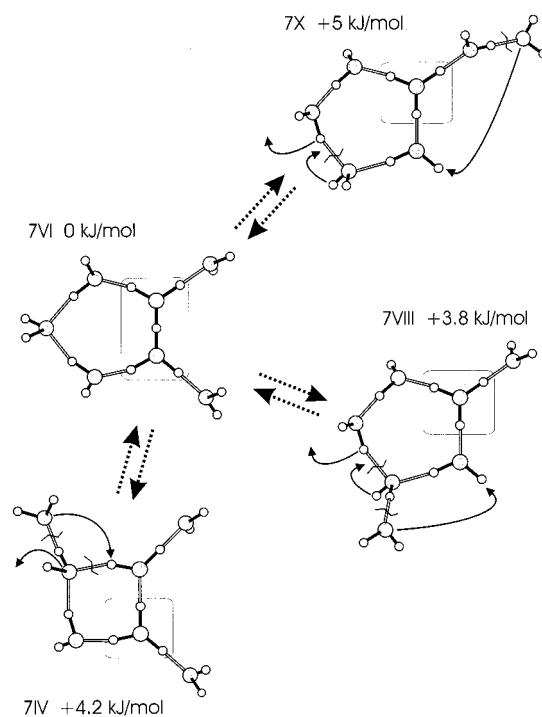


**Figure 6.** Computed relative enthalpies of several  $\text{H}^+(\text{H}_2\text{O})_7$  isomers and possible pathways of their interconversion. Note that the core ion changes from  $\text{H}_3\text{O}^+$  to  $\text{H}_5\text{O}_2^+$ —the Eigen and Zundel cations, respectively—and vice versa. (Adapted from data of ref 143).

immediately forming a strongly bound  $\text{H}_3\text{O}^+$  hydronium ion with  $\text{H}^+$ , and this ion has been extensively studied also, both by experiment and theory. Again, in an essential agreement, it is found to be a symmetric  $C_{3v}$  entity, with the charge equally distributed between the three equivalent hydrogen atoms. One therefore has an alternative model of the proton in water: solvated  $\text{H}_3\text{O}^+$ , as proposed many years ago by Eigen; when aqueous reactions involving a proton are considered, they are often formulated as reactions of  $\text{H}_3\text{O}^+$ .

A large number of theoretical studies appeared investigating both the structure and local charge center geometry in aqueous solutions as well as proton diffusion dynamics. After reviewing this vast literature, one comes to realize that the results are inconclusive, and while some studies lean toward the  $\text{H}_5\text{O}_2^+$  structures for the aqueous proton,<sup>129–132</sup> others find  $\text{H}_3\text{O}^+$ <sup>133–136</sup> preferable. In general, most calculations, including DFT work in our group, indicate that the difference between the two geometries is relatively small, sensitive to the computational method used, and strongly affected by the surrounding hydrogen-bonded network.<sup>137–142</sup> One then has to consider the dynamic nature of the problem, the fact that in liquid water the hydrogen bonds are constantly broken and reformed. Moreover, the proton in water is not localized but the charge moves efficiently through the solution, and the situation is highly fluxional (see Figure 7). One can therefore not really speak about rigid ions, and the question of structure becomes somewhat semantic. One can, however, still ask which of the two models is a better approximation in view of the experimental observations.



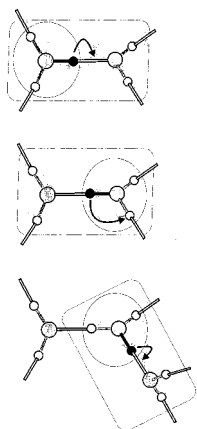


**Figure 7.** Proton transfer and charge motion in water. The proton, lacking electrons, is essentially a point charge and prefers to bind two and only two ligands.<sup>173</sup> While an isolated gas-phase  $\text{H}_3\text{O}^+$  cation is a symmetric  $C_{3v}$  ion, in solution it will tend to distort and form transiently  $\text{H}_5\text{O}_2^+$  “Zundel”-type structures with neighboring molecules. The  $\text{O}-\text{H}^+-\text{O}$  potential will, in general, be asymmetric, fluxional, and depend on the residual instantaneous state of solvation of the  $\text{H}_5\text{O}_2^+$  entity. These transient  $\text{H}_5\text{O}_2^+$  subunits may be considered transition states for transfer of a proton from one water molecule to another. Through repeated proton transfer of this type, the charge can move freely through the liquid without actual long-range motion of its atoms.

The strong hydrogen bonding and constant motion make a precise determination of the structure of liquid water difficult, and most experimental techniques will yield structures averaged over time and space. The easy mobility of protons in aqueous systems might, however, be viewed as evidence for the importance of the Eigen model. While one can easily model the diffusion of protons by moving across the asymmetric  $\text{H}_2\text{OH}\cdots\text{OH}_2$  bond from one water molecule to another, resulting in motion of the hydronium ion entity, it is more difficult to model the motion of a proton locked in a symmetric bond between two strongly bound water ligands. Obviously, the transition state for proton transfer from a hydronium ion to a nearby water molecule will have a geometry resembling the Zundel cation.

The stability of ionic water clusters, including our studies of blackbody fragmentation of hydrated protons, also provides some insight into this question. As noted above, the absorption of photons from the blackbody wall radiation by the water clusters results in their heating and fragmentation. Evaporation of each ligand then cools the cluster again and this cycle repeats itself. The process ends when the clusters reach the wall temperature, i.e., when the rate of heating by photon absorption is identical to the rate of cooling by photon emission, and when all the remaining ligands are so strongly bound that the rate of their loss at ambient temperature is negligible on the time scale of the experiment.

If the strongly bound symmetric  $\text{H}_5\text{O}_2^+$  Zundel cations were the key structures for hydrated protons, one might expect the process of  $\text{H}^+(\text{H}_2\text{O})_n$  to stop at  $n = 2$ , leaving behind the stable  $\text{H}_5\text{O}_2^+$  ion, or possibly at  $n = 6$ , with all four peripheral hydrogens of the Zundel cation being symmetrically solvated by

water molecules. Experimentally, the fragmentation stops clearly and abruptly at  $n = 4$ , which corresponds to a symmetrically solvated hydronium,  $\text{H}_3\text{O}^+(\text{H}_2\text{O})_3$ . The  $n = 5$  cluster exhibits no special stability and still fragments quite efficiently, while essentially no further ligand loss is detectable for  $n = 4$ , and its fragmentation must be at least an order of magnitude slower. The measured proton hydration enthalpies tell a similar story. By far, largest is the first hydration enthalpy  $\Delta H = 693$  kJ/mol, which results in the hydronium ion. The enthalpy for hydration with a second water molecule, forming the symmetric Zundel ion, is nearly a factor of 5 smaller, 127.6 kJ/mol, and not that different from the third and fourth hydration enthalpies. Hydration with four waters corresponds to the fully solvated hydronium ion. After  $n = 4$ , there is another sharp drop of about a factor of 2 in the hydration energies, with the fifth and the following hydration enthalpies remaining almost constant around 35 kJ/mol.

To summarize, it seems that if one wishes to formulate the aqueous proton as a discrete ion, the description in terms of the hydronium  $\text{H}_3\text{O}^+$  “Eigen” ion, as mostly used in the literature, provides a much better agreement with the experimental evidence and observations than invoking the  $\text{H}_5\text{O}_2^+$  species. Since, however, as noted above, the preferred configuration around the charged center is strongly affected by the hydrogen-bonded network in its neighborhood, the question remains if clusters where the hydrogen-bonded network is finite can be described in terms of a solvated  $\text{H}_3\text{O}^+$  or if “Zundel” structures will also be important. Ab initio calculations on small ionic water clusters, in fact, indicate in many cases a number of structural isomers often with low interconversion energies, where the energy differences between the hydrated “Zundel” and “Eigen” ion structures depend strongly on the overall number of ligands  $n$  and on the rest of the hydration network<sup>143</sup> (see also Figure 6).

#### IV. Water Clusters as a Medium for Aqueous Reactions

Above we have already pointed out how strongly the properties of atoms and molecules are affected by the solvent and to what extent the solution can affect their chemistry. This is especially true of water, which due to the highly polar nature of its molecules and its ability to form strong hydrogen bonds significantly stabilizes ions and polar structures. Thus, hydrogen halides, whose ionization in the gas phase requires a large energy input, ionize spontaneously in aqueous solution with development of heat, and even triply ionized ions such as  $\text{Fe}^{3+}$  or  $\text{Al}^{3+}$  ions, whose production in the gas phase would require over 50 eV, are quite common and stable in aqueous solutions.

The blackbody fragmentation of water clusters provides a convenient tool for successively removing the stabilizing water molecules from the system of interest one by one and for investigating in this way, in detail, the effect of the solvent upon the solute structure and upon the processes occurring in the solution.

## A. Reduction–Oxidation Processes in Water Clusters

Water clusters containing magnesium ions were extensively studied both in molecular beams<sup>140,17</sup> and trapped in an FT-ICR trap,<sup>41,42</sup> with all studies reporting similar observations. Depending somewhat on the exact experimental conditions of the laser vaporization source used to produce the clusters, two different types of ions are observed. Aggregates of the composition  $\text{Mg}^+(\text{H}_2\text{O})_n$  are observed for  $n = 1-6$  and also for  $n \geq 17$ . On the other hand, in the range  $6 \leq n \leq 16$ , the clusters exhibit almost exclusively a  $\text{MgOH}^+(\text{H}_2\text{O})_n$  composition. This suggests strongly that the magnesium atoms occur in these clusters in at least two different oxidation states. While the latter clusters almost certainly contain  $\text{MgOH}^+$ , magnesium hydroxide cations with divalent magnesium, there is little doubt that at least the small  $\text{Mg}^+(\text{H}_2\text{O})_n$  contain a singly ionized magnesium atom.

Interesting further insights are provided by an FT-ICR experiment, where very large clusters  $\text{Mg}^+(\text{H}_2\text{O})_n$  are produced and then allowed to fragment by the blackbody radiation. They first sequentially lose water ligands one by one, but when the number of water ligands is reduced to about  $n = 17-20$ , an interesting process takes place. Instead of “evaporating” a further water molecule, a chemical reaction within the cluster apparently takes place, the magnesium is converted to hydroxide, and a hydrogen atom is lost



perhaps with a concurrent loss of an additional water ligand. Clearly a reduction–oxidation process takes place in the cluster, with magnesium seemingly being oxidized to  $\text{Mg}^{2+}$  and a water molecule reduced to yield a hydrogen atom.

The process is easier to understand if one recalls that magnesium cation,  $\text{Mg}^+$ , is isovalent with neutral Na. Sodium and other alkali metals readily dissolve in strongly polar solvents, e.g., ammonia, to yield deep blue solutions, which are as previously noted now well-known to contain  $\text{Na}^+$  ions and solvated electrons. The question therefore arises if the magnesium is being oxidized to  $\text{Mg}^{2+}$  at the moment when the hydroxide forms and a hydrogen atom is lost or if the large clusters with  $n > 17$  already contain the doubly charged ion and a free electron. One could then postulate that as the quantity of the stabilizing solvent drops below some critical limit, the cluster can no longer accommodate both the closed-shell  $\text{Mg}^{2+}$  ion and an electron and they recombine forming the much more reactive, open-shell  $\text{Mg}^+$  ion. This in turn would then react with a water molecule forming hydroxide and eliminating the hydrogen atom (cf. Figure 8). The group of Fuke demonstrated using a laser photofragmentation experiment<sup>144</sup> that the very small,  $n < 5$ , clusters absorb in the region of the expected, fully allowed  $2s-2p$  transition and therefore probably contain the open-shell  $\text{Mg}^+$  ion. It would be very interesting to perform a similar experiment for the large  $n > 20$  clusters and show if this absorption is absent.

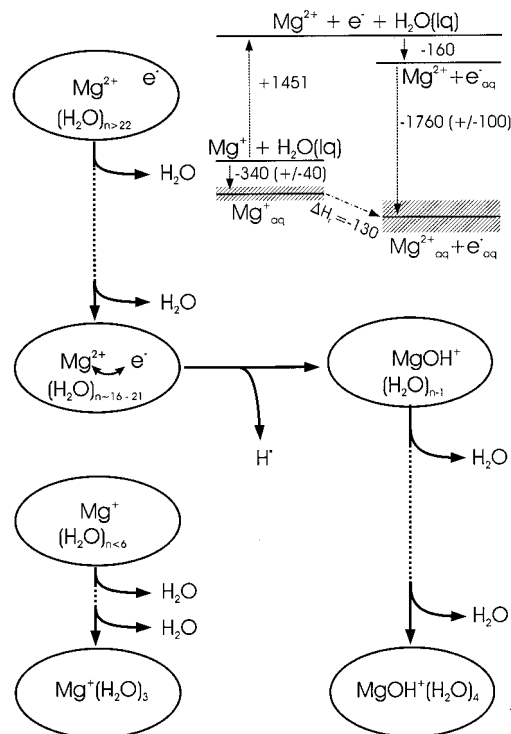


**Figure 8.** Hydrated  $\text{Mg}^+(\text{H}_2\text{O})_n$  cluster fragmentation. As suggested in the text, large clusters contain presumably separately hydrated  $\text{Mg}^{2+}$  and  $e^-$ . They lose water ligands until a critical size range of  $n \approx 16-21$ . When the amount of solvent becomes insufficient to stabilize the two separate charges, the electron recombines with  $\text{Mg}^{2+}$ . The open-shell  $\text{Mg}^+$  instantly reacts with a nearby water molecule, yielding magnesium hydroxide cation and a hydrogen atom, which evaporates from the cluster. The inset shows using estimated hydration enthalpies that in a bulk solution  $\text{Mg}^+$  should lie higher in energy than  $\text{Mg}^{2+} + e^-_{\text{aq}}$ .<sup>42</sup>

Very similar processes were also observed in clusters containing the  $\text{Ca}^+$  and  $\text{Al}^+$  cations. While the reactions in the calcium case<sup>145</sup> are quite analogous to those of magnesium, the chemistry of trivalent aluminum requires some modification.<sup>11,41,124</sup> As in the magnesium case, in the aluminum case one also observes several regions where ions of different compositions are preferred. For  $n < 12$  as well as  $n \geq 24$ , hydrated  $\text{Al}^+$  ions,  $\text{Al}^+(\text{H}_2\text{O})_n$  dominate. In the intermediate range, on the other hand, one observes predominantly aluminum hydroxide clusters,  $\text{Al}(\text{OH})_2 + (\text{H}_2\text{O})_n$ , but the boundaries between the ranges are somewhat more diffuse than in the magnesium case.

Also, the fragmentation of the clusters shows similarities to the magnesium case. The small  $n < 12$   $\text{Al}^+(\text{H}_2\text{O})_n$  clusters simply lose one water ligand at a time, resulting after about 120 s predominantly in tetrahydrates,  $\text{Al}^+(\text{H}_2\text{O})_4$ , which then only extremely slowly lose additional water molecules. It appears to be fairly clear that these hydrates indeed contain the singly ionized, closed-shell  $3s^2\ ^1S$   $\text{Al}^+$  ion. Similarly, the hydroxide ions also lose stepwise water ligands, ending up eventually predominantly as the  $\text{Al}(\text{OH})_2^+(\text{H}_2\text{O})_3$  ion, i.e., the dihydroxy cation of  $\text{Al}^{3+}$  solvated by three additional water ligands. When, however, one allows the larger solvated  $\text{Al}^+$  ions to fragment, a more complex intracluster chemistry apparently occurs. This results in the formation of

hydroxide and a release of, in this case, molecular hydrogen



Again, a redox process takes place, with aluminum in a trivalent  $\text{Al}^{3+}$  state and with molecular hydrogen being formed. In this case a two-electron exchange takes place, with aluminum going from a closed-shell singly ionized form again to a closed-shell triply ionized valence state, consistent with the tendency of the third group elements to occur in their compounds to be either trivalent or monovalent.

It is again not trivial to decide if the oxidation of the aluminum atom is concurrent with the hydrogen evolution or if "pre-formed"  $\text{Al}^{3+}$  ions already exist in the large hydrated clusters. While in magnesium the energetics seem to favor second ionization in water, in the case of aluminum the solvation energies of the  $\text{Al}^{3+}$  ion and of two electrons seem to fall somewhat short of the energy needed to form the ion, the sum of the second and third ionization potentials.<sup>41</sup> On the other hand, if one considers that the three charges will not be removed to an infinite distance and takes into account the stabilization by the screened Coulombic potential between the electrons and  $\text{Al}^{3+}$ , then the possibility of the triply ionized Al being present in the cluster cannot be a priori dismissed.

## B. Multiply Ionized Clusters

In the above paragraphs we have postulated that the large hydrated  $\text{Mg}^+$  clusters may actually involve  $\text{Mg}^{2+}$  and a solvated electron, but in the absence of a real spectroscopic structural study, the evidence is indirect. On the other hand, the stability of doubly or even triply ionized metal cations in bulk aqueous solutions is a well-established fact. While our laser vaporization source in the present form does not generate observable concentrations of doubly charged cations, these can be, and were, produced by means of, for instance, electron ionization or by electrospray methods, as demonstrated in the pioneering work of Kebarle and co-workers, and studies of their stability are a topic of considerable interest.<sup>146,147</sup>

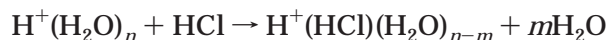
Although ions of the type  $\text{M}^{2+}(\text{H}_2\text{O})_n$  are undoubtedly almost in all cases thermodynamically unstable with respect to charge or proton transfer followed by Coulombic explosion, they can be generated and leisurely studied by mass-spectroscopic means. A recent theoretical investigation of the rare-earth cations with  $n = 2$  by DFT techniques revealed that the ions are separated from the  $\text{MOH}^+ + \text{H}_3\text{O}^+$  global minimum by two potential barriers.<sup>148</sup> The first higher barrier involves moving one of the water ligands from the first to the second solvation shell and is almost equal to the energy needed to completely break the bond between the doubly charged cation and the water ligand. The second activation barrier then represents a proton transfer from the first solvation shell water to the one in the second solvation shell, resulting in an  $\text{M}^{2+} \cdot \text{OH}^- \cdot \text{H}_3\text{O}^+$  "salt bridge" structure, which then smoothly dissociates into hydroxide and hydronium cations.

An interesting recent experimental study of hydrated doubly ionized zinc cations was reported by Peschke et al.<sup>147</sup> They found that the reaction of  $\text{Zn}^{2+}(\text{H}_2\text{O})_n$  ( $n = 8, 9$ ) with ammonia results in a proton transfer and fission of the cluster, resulting in a hydrated  $\text{ZnOH}^+$  and hydrated  $\text{NH}_4^+$ . Apparently the higher proton affinity of ammonia is sufficient to destabilize the hydrated  $\text{Zn}^{2+}$  ion and overcome the barrier to proton transfer. Future studies of multiply charged ions in an ICR instrument should be a very fruitful area and, in particular, combined with spectroscopy will undoubtedly yield very interesting results and insights into aqueous ion solvation.

## C. Ionic Dissolution, Neutralization, and Precipitation Reactions in Water Clusters

Even though the collision-free, blackbody, fragmentation of the clusters described in the previous section provides some interesting insights, at least equally interesting information can be gained by increasing the pressure in the ICR-cell region by actively introducing suitable reactants and observing binary collisional processes and true chemical reactions of the hydrated clusters. The introduction of an inert gas such as helium or argon at first has little effect and the pressure has to be increased by 2 orders of magnitude above the  $10^{-9}$  Pa ( $10^{-11}$  Torr) baseline range before the collisional processes can compete with the blackbody fragmentation and slight increases in the fragmentation rates become observable. The inert gases interact with the ionic clusters much more weakly than the polar water ligands, and their incorporation into the clusters is not detected.

It should naturally be much more interesting to introduce reactive molecules into the system and investigate true chemical reactions initiated by their binary collisions with clusters. As an example, one can let the hydrated proton clusters interact with hydrochloric acid, which is well-known to react avidly with bulk water and dissolve in it exothermically with ionization. Upon introducing hydrochloric acid into the spectrometer, one finds that the HCl molecules are very efficiently exchanged for the water ligands, with the reaction being, however, strongly size-dependent

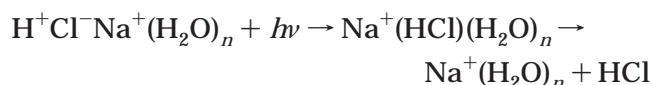


There appear to be clear limits to the "solubility" of HCl in water clusters, such that, for instance, clusters with  $n < 9$  do not react with HCl at all. Allowing the reactions to proceed for a longer time, one finds that the clusters  $9 \leq n \leq 13$  can dissolve at most one molecule of hydrochloric acid and those with  $n > 13$  two, and similarly, one can find limits to the "solubility" for even larger clusters. Conversely, when one allows the large clusters "saturated" with HCl to fragment, they gradually lose water, but whenever one of the above limits is reached, a hydrochloric acid molecule is lost instead. The reason clearly is that as in a bulk aqueous solution, the HCl in the cluster does not remain covalently bound but dissociates ionically. This is, however, only possible, when enough solvent is available to stabilize the ions. As the



number of solvent ligands drops upon fragmentation below some critical level, the covalent hydrochloric acid molecule becomes energetically more favorable and the  $\text{H}^+$  and  $\text{Cl}^-$  ions recombine. Unlike  $\text{H}_2\text{O}$ , the  $\text{HCl}$  molecule has only one proton with which to form a hydrogen bond, therefore bound more weakly and evaporates preferentially from the cluster. The limited solubility of hydrochloric acid in water clusters and even the observed quantitative limits seem to be in fair agreement with the nice theoretical calculations of Agmon and co-workers on concentrated  $\text{HCl}$  solutions,<sup>149</sup> as well as with the recent studies of  $\text{HCl}$  uptake by protonated water clusters in a flow reactor under equilibrium conditions.<sup>150,151</sup>

The above examples show that hydrated clusters can be considered to be miniature "nanosolutions", miniature droplets in which polar reactants can be ionically dissolved and a variety of ionic reactions studied. One can, for instance, use the dissolution of an acid, e.g.,  $\text{HCl}$  or  $\text{HBr}$ , to neutralize a base cation, for instance,  $\text{Na}^+$  present in the cluster, resulting in a cluster with "dissolved" chloride or bromide.<sup>12</sup> Interestingly, one again finds that this "neutralization" only works for clusters above some critical size, with  $\text{Na}^+(\text{H}_2\text{O})_n$  clusters below  $n \approx 12$  not reacting with hydrogen halides at all; apparently at least 12 water ligands are needed to stabilize the three ions in the solution:  $\text{H}^+$  (or  $\text{H}_3\text{O}^+$ ),  $\text{Na}^+$ , and  $\text{Cl}^-$ . When larger clusters with dissolved  $\text{HCl}$  (or  $\text{HBr}$ ) are allowed to fragment, as soon as the amount of solvent drops below this  $n \approx 12$  limit, the  $\text{H}^+$  and  $\text{Cl}^-$  ions again recombine and hydrogen chloride (bromide) evaporates from the cluster (Figure 9, top spectrum)



Similar "neutralization" reactions can naturally also be carried out with clusters containing group II or III metals, e.g., magnesium or aluminum. In clusters of the "hydroxide" variety, e.g.,  $\text{MgOH}^+(\text{H}_2\text{O})_n$ , a true neutralization takes place. The hydroxyl anion apparently recombines with the proton, with the reaction heat resulting in the evaporation of one or two molecules of water,<sup>42</sup> and one observes product ions of the type  $\text{MgCl}^+(\text{H}_2\text{O})_{n-m}$ . Quite analogous is also the reaction of the aluminum hydroxide clusters, except that here the neutralization and replacement of the hydroxyls must occur sequentially in two steps,  $\text{Al}(\text{OH})_2^+(\text{H}_2\text{O})_n \rightarrow \text{Al}(\text{OH},\text{Cl})^+(\text{H}_2\text{O})_m \rightarrow \text{AlCl}_2^+(\text{H}_2\text{O})_k$ , with an intermittent formation of chloride-hydroxide.<sup>124</sup>

Particularly interesting are the reactions of the hydrated metal clusters, e.g., ions of the  $\text{Al}^+(\text{H}_2\text{O})_n$  type. Here again the primary step is apparently ionic dissolution of the hydrochloric acid in the water cluster, and this is followed by a reaction of the acid with the metal with evolution of molecular hydrogen<sup>11</sup>

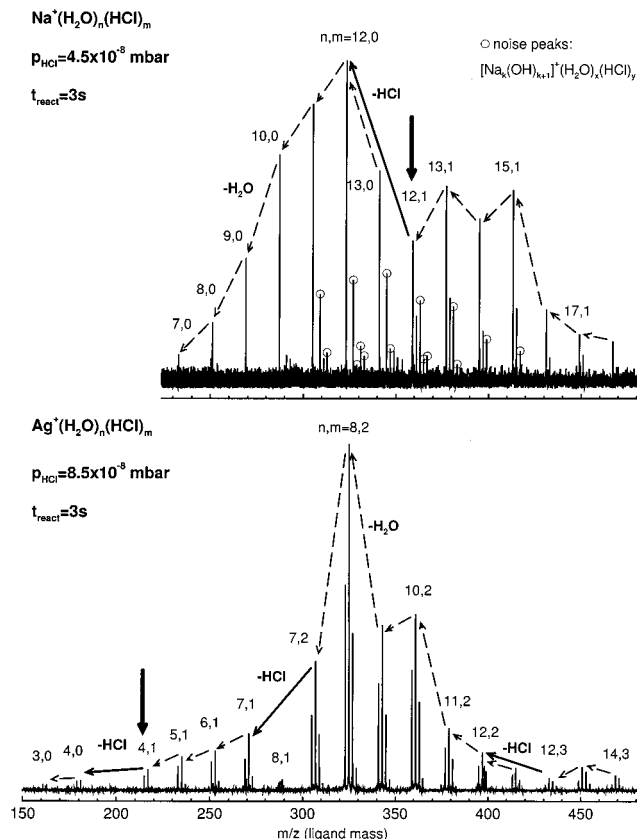
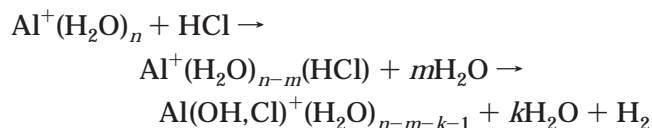


**Figure 9.** Mass spectra contrasting the reactions of  $\text{HCl}$  with hydrated  $\text{Na}^+$  and  $\text{Ag}^+$ . Hydrated  $\text{Na}^+(\text{H}_2\text{O})_n$  in the top spectrum "dissolve"  $\text{HCl}$  only for  $n > 13$ , since enough solvent is needed to stabilize three separate ions,  $\text{Na}^+$ ,  $\text{H}^+$ , and  $\text{Cl}^-$ . This limit shifts in  $\text{Ag}^+(\text{H}_2\text{O})_n$  in the bottom spectrum to  $n = 4$ , since the insoluble  $\text{AgCl}$  "precipitates" out of the solution, and only one ion,  $\text{H}^+$ , needs to be stabilized by the solvent.<sup>12</sup>

For smaller values of  $n$ , the second step is almost immediate, but for hydrates above  $n \approx 25$ , the intermediate  $\text{Al}^+(\text{H}_2\text{O})_n(\text{HCl})$  products with dissolved  $\text{HCl}$  and prior to  $\text{H}_2$  elimination are stable long enough to be detected. From the relative intensity of the corresponding mass peaks one can estimate their lifetime to be about 100 ms. Again in subsequent collisions with  $\text{HCl}$  the second  $\text{OH}$  anion is also replaced by chloride, resulting in  $\text{AlCl}_2^+(\text{H}_2\text{O})_n$  product ions.

The fact that the primary step is the ionic dissolution of the acid is confirmed by the experimental observation that again the reaction of the  $\text{Al}^+(\text{H}_2\text{O})_n$  with  $\text{HCl}$  exhibits a lower limit of about  $n = 11$ . Clusters with  $n < 11$  simply collisionally fragment but do not chemically react with the hydrochloric acid at all. The hydrogen evolution observed in the large clusters can essentially be viewed as a proton-catalyzed metal oxidation and its dissolution in acid. In the absence of a sufficient number of water ligands to ionically dissolve the hydrochloric acid, the aqueous proton cannot form and the reaction cannot proceed.

An interesting situation arises when the basic cation present in the cluster and the anion of the reactant acid form a highly insoluble product, which would normally precipitate from a bulk solution. This is, for instance, the case in the reaction of  $\text{Ag}^+(\text{H}_2\text{O})_n$

clusters with hydrogen halides, HCl or HBr, which is exemplified by the bottom spectrum in Figure 9. The reactions here are quite similar to those observed with, for instance,  $\text{Na}^+$ ; however, the minimum sizes for the reaction to occur are in this case shifted.<sup>12</sup> When larger clusters with “dissolved” hydrochloric acid are allowed to fragment, the last HCl molecule does not evaporate around  $n = 12$ , as in the sodium case, but only around  $n = 4$ . The reason is that a  $\text{Na}^+(\text{H}_2\text{O})_n$  with a dissolved HCl has to hydrate and accommodate three ions:  $\text{Na}^+$ ,  $\text{H}^+$ , and  $\text{Cl}^-$ , and this, as shown above, apparently requires at least 12 water ligands. In the case of the  $\text{Ag}^+$  ion reaction, the insoluble  $\text{AgCl}$  “precipitates” out of the solution (to the extent one can talk about precipitation of a single molecule) so that just a single proton needs to be solvated.

In connection with insoluble inorganic salts, it might still be mentioned that attempts to react solvated metal cations with gaseous  $\text{CO}_2$  and “precipitate” insoluble carbonates yielded negative results. The investigation revealed that the hydrated  $\text{Ba}^+$  and  $\text{Mg}^+$  cations exhibit no chemical reaction with  $\text{CO}_2$  on the time scale of the experiment. The precipitation of the carbonate apparently first requires dissolving the carbon dioxide and formation of a carbonate anion. The “solubility” of  $\text{CO}_2$  in the clusters is apparently too small, and the only observed process is a collisional fragmentation and a gradual loss of water ligands.

#### D. Acid and Basic Clusters and Catalytic Processes

When considering chemical reactions of the hydrated clusters, it is useful to remember that, for instance, a hydrated  $\text{H}^+(\text{H}_2\text{O})_n$  cluster with  $n \approx 55$  water ligands has approximately the same relative  $\text{H}^+$  concentration as a strongly acid solution with  $\text{pH} = 0$  and similarly an  $\text{OH}^-(\text{H}_2\text{O})_n$  cluster with a similar number of ligands has a hydroxyl ion concentration of a basic bulk solution with  $\text{pH} = 14$ . We have already pointed out that indeed the clusters behave in their reactions as a strongly basic or strongly acid medium. Thus, the evolution of hydrogen in solvated metal cations is effectively a proton-catalyzed process, and similarly ions containing, e.g.,  $\text{Al}^+(\text{OH})_2$  cations can be neutralized by acids to yield chloride or bromide salts.

The analogy with bulk solutions goes, however, beyond simple inorganic reactions of the water clusters. Also, numerous organic reactions are known to be acid- or base-catalyzed, i.e., they proceed with greatly enhanced rates in strongly acid or basic solutions. While the detailed mechanisms of such reactions vary and depend on the specific reactants, the fundamental reason for the increased rate is common to all: an ion, be it  $\text{H}^+$  or  $\text{OH}^-$ , binds to one of the reactants and a neutral–neutral reaction is thus converted to a much more efficient ion–neutral process. In principle, one could expect that such a coupling between the neutral reactant and the  $\text{H}^+$  or  $\text{OH}^-$  could take place equally well in the finite cluster as in the bulk.

A well-known example of such a process is the so-called “aldol condensation”, which is known to be in

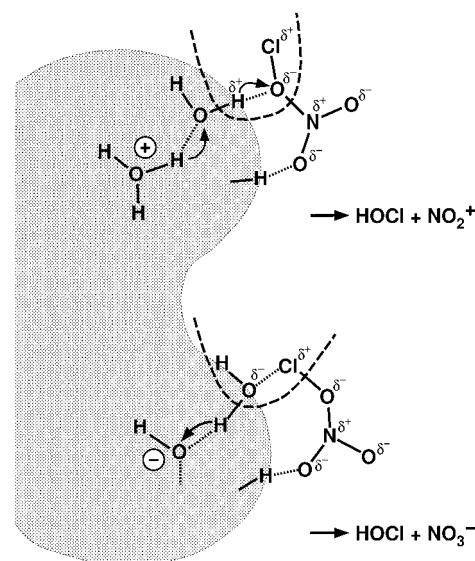


**Figure 10.** Both “acidic” and “basic” water clusters react with  $\text{ClONO}_2$ , releasing hypochlorous acid,  $\text{HOCl}$ , into the gas phase and leaving an  $\text{NO}_2^+$  or  $\text{NO}_3^-$  ion, respectively, within the cluster. The nearly 100% reaction probability per collision of the anionic “basic” process suggests that this is more important than the cationic “acid” reaction, which is about a factor of 20 less efficient.<sup>161</sup>

aqueous medium preferentially base-catalyzed.<sup>152</sup> The reaction shown schematically in Figure 12 involves a coupling of two organic compounds containing carbonyl groups—aldehydes or ketones. In this reaction, the  $\alpha$ -CH group of one of the molecules is essentially added across the CO double bond of the other, which results in linking of the two molecules via a new C–C bond. For instance, in the simplest case, when the reactants are two acetaldehyde molecules, a  $\text{C}_4$  molecule with both an aldehydic and an alcoholic group, a so-called aldol, results, and this reaction proceeds very efficiently in strongly basic bulk aqueous solutions. One can thus try to use the large water clusters as the reaction medium, “dissolve” the acetaldehyde (or acetone) reactant, “evaporate” the solvent, and examine the products.

When large water clusters are reacted, one finds that indeed acetaldehyde (or acetone) molecules undergo an efficient ligand exchange against the water molecules and the carbonyl compound molecules can be “dissolved” in the cluster. Starting with the “acidic”  $\text{H}^+(\text{H}_2\text{O})_n$  clusters, the final product of a long series of ligand-exchange and fragmentation reactions is just a proton solvated by 2–3 aldehyde molecules but with no “real” chemical reaction having taken place, with no existing covalent bonds having been broken, or new ones formed.

When, on the other hand, the “basic”  $\text{OH}^-(\text{H}_2\text{O})_n$  clusters are used as the reaction “medium”, a true chemical reaction takes place. Similar to bulk basic solutions, the final product of the reaction and fragmentation can be identified as an aldolate anion, i.e., effectively two acetaldehyde molecules linked via a new C–C covalent bond between the carbonyl group of one of the acetaldehydes and the methyl group of the other. In the process not only are all of the original water ligands lost, but also an additional hydrogen which originates from one of the acetalde-

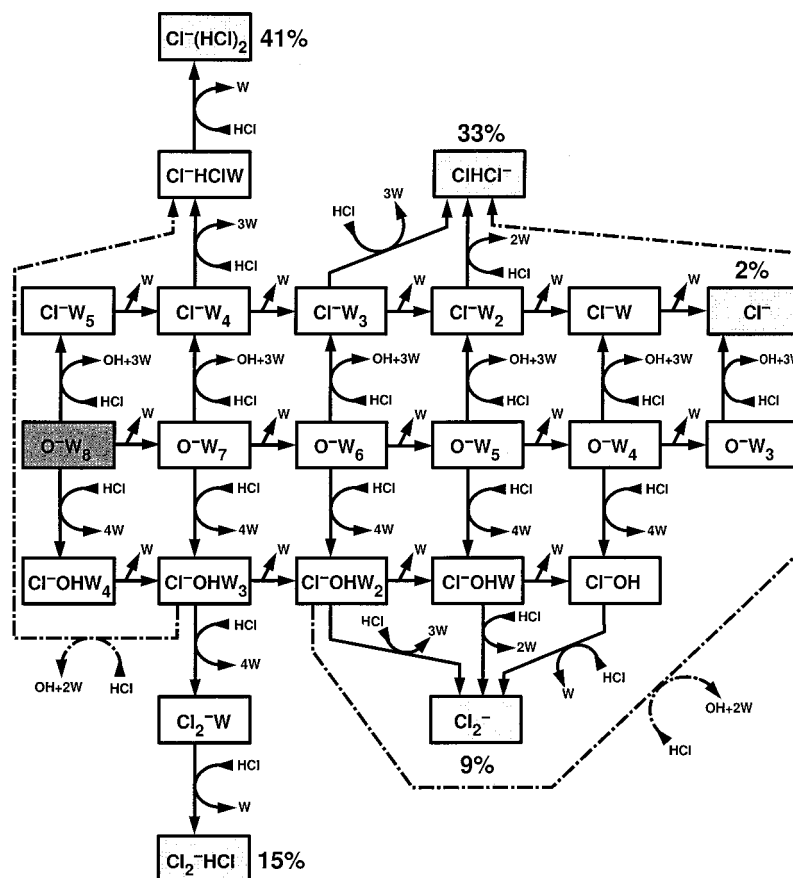


**Figure 11.** Anionic cluster reactions with HCl. As exemplified by the size-selected  $\text{O}^-(\text{H}_2\text{O})_8$ , hydrated anionic clusters exchange due to the high electron affinity of chlorine water ligands efficiently for HCl, resulting in a solvated chloride anion. Eventually all water ligands are lost, with  $\text{Cl}^-(\text{HCl})_n$ ,  $n = 0-2$ , being the products. At longer times, the bialide anion,  $\text{HCl}_2^-$ , is the major product with a minor parallel reaction channel forming  $\text{Cl}_2^-$  anions.<sup>123</sup>

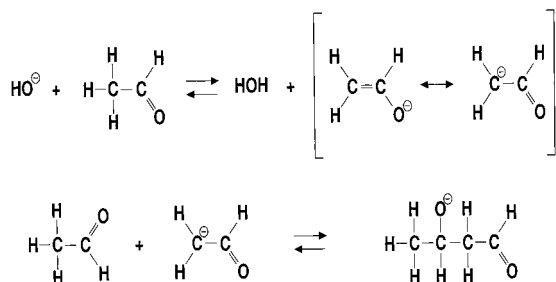


**Figure 12.** Acid–base catalysis in ionic water clusters: condensation of two acetaldehyde molecules in  $\text{OH}^-(\text{H}_2\text{O})_n$  clusters results in an aldolate anion, the same way it occurs in strongly basic solutions. Isotopic experiments confirm that the lost atom is not the aldehydic hydrogen but originates from the methyl group. They also show that the top reaction proceeds reversibly back and forth, resulting in isotopic exchange of the methyl hydrogens with the solvent.<sup>152</sup>

hyde molecules. This shows that besides a new chemical bond being formed, also a CH bond was broken. Interestingly, one can show by selective isotopic substitution of the acetaldehyde that the hydrogen atom lost does not originate from the aldehydic group but from the methyl<sup>152</sup> (cf. Figure 12). In addition, with the deuterated compound experiments one also finds that interesting and efficient isotopic exchange reactions between the methyl hydrogen atoms on the carbonyl compound and the water solvent protons take place. The aldol

condensation reaction in clusters is naturally not restricted to acetaldehyde but proceeds similarly, for instance, in acetone and undoubtedly in other compounds containing a carbonyl group.

### E. Reactions of Water Clusters with Polar Organic Molecules: Hydrophobic and Hydrophilic Interactions

Quite some time ago Kebarle and co-workers investigated the reactions of hydrated proton clusters with several polar organic molecules, including dimethyl ether.<sup>153</sup> Ethers can be viewed as substituted derivatives of water and possess a number of interesting properties. Their oxygen atom can be the acceptor part of a hydrogen bond, but unlike water, they have no OH groups and cannot form donor hydrogen bonds. Ethers also have appreciable dipole moments, with a hydrophilic and hydrophobic end, and unlike some of the compounds examined above, e.g., HBr or NaCl, they have only a limited solubility in water.

Similar reactions can very conveniently and in considerable detail be investigated by the FT-ICR technique. Such studies of the reactions of large  $\text{H}^+(\text{H}_2\text{O})_n$  clusters up to  $n \approx 75$  with diethyl ether<sup>154</sup> have revealed a very efficient exchange of the ether molecules for the water ligands. At an initial stage of the reaction a large variety of products is formed, so that after a short time (about 3 s at a pressure of



$\approx 10^{-5}$  Pa) a very complex product pattern is observed. After a somewhat longer time, however, these mass spectra are appreciably simplified, with predominantly only a relatively small number of apparently more stable product clusters remaining. These more stable ions have the composition  $\text{H}^+(\text{H}_2\text{O})_m\text{-Et}_{m+2}$  with up to  $m \approx 5\text{--}6$ . These then slowly further fragment, so that after about 15 s,  $m = 1$  becomes the most abundant ion. After a sufficiently long time, even this ion breaks up, and after about 30 s, mainly the final  $m = 0$  product, which is stable under the conditions of the experiment, remains.

It is interesting to consider the structure of this set of ions with increased stabilities. The  $m = 1$  ion is clearly a hydronium cation,  $\text{H}_3\text{O}^+$ , with each of its protons hydrogen-bonded to an oxygen atom of an ether molecule. One can also easily understand the structure of the  $m = 4$  aggregate with four  $\text{H}_2\text{O}$  molecules as being a hydronium ion solvated with a water molecule bound to each of its three protons. This then leaves six peripheral protons on the three water ligands, each of which again accommodates one ether molecule. In general, each of the preferentially stable ions represents a network of a few hydrogen-bonded water molecules with each of the remaining dangling OH groups being bound to an ether molecule. In principle, these species are a cluster of hydrogen-bonded species, which owes its preferential stability to a closed hydrophobic solvation shell protecting them from attack by other polar ether or water molecules.

One might perhaps note that the principle of stabilizing the clusters by a hydrophobic shell is in some respects similar to the forces stabilizing, for instance, micelles in bulk solutions. The hydrophobic repulsions also represent one of the types of interactions important in stabilizing cells and other biological systems. With a suitable choice of surfactants, it might not be without interest to investigate the stability and reactions of micelle-like structures in an FT-ICR mass spectrometer.

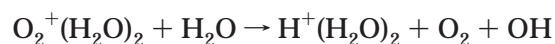
Another point worth mentioning is that from the above-mentioned group of particularly stable ions, the  $m = 2$  one is easily recognized as the previously discussed Zundel cation, i.e., an  $\text{H}_2\text{O}\cdot\text{H}^+\cdot\text{OH}_2$  ion, with four ethyl ether molecules terminating the dangling OH groups. Unlike the hydrated hydronium, the  $m = 1$  ion, which in the course of the fragmentation process remains the most abundant ion for a relatively long time, the  $m = 2$  species exhibits no particular stability. At no time is it the most abundant ion, and its stability seems to be comparable to that of, for instance, the larger  $m = 3$  or 4 species. This again supports the notion that the "Eigen" hydronium cation provides a much more useful concept and description of the positive charges in aqueous solutions than the "Zundel" ion, as already discussed in one of the previous sections.

As a final remark, one might note that eventually all water ligands are lost and the final product of fragmentation is the  $m = 0$  ion, i.e., a proton solvated by two ether ligands. This simply reflects the fact that diethyl ether with its higher proton affinity than water eventually wins the competition for the proton.

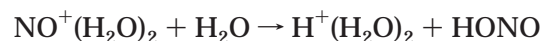
## F. Water Clusters as Model Systems for Atmospheric Reactions

Even though ions represent only a very minute fraction of the atmosphere, they have a disproportionate influence on many atmospheric phenomena. Ions occur in the atmosphere with relatively high abundance only at altitudes above  $\approx 60$  km, and water and hydration play important roles in their chemistry. In the atmosphere there are several sources of ionization; at higher levels, in the so-called E and F regions (above  $\approx 90$  km), extreme solar UV and X-rays are the major causes of ionization. Below about 60 km, galactic cosmic rays and even lower in the troposphere radioactive decay are the prevailing ion sources. The open-shell oxides of nitrogen, NO and  $\text{NO}_2$ , have among the common components of the atmosphere the lowest ionization potentials, and indeed Lyman- $\alpha$  ionization of NO as well as metastable  $^1\Delta_g \text{O}_2$  become the most important sources of ions in the so-called D region (70–90 km).

Investigations of the abundance of ions in the atmosphere led to the interesting observation of a sharp boundary at around 85 km. Above this altitude one indeed finds that  $\text{NO}^+$  as well as  $\text{O}_2^+$  ions dominate. Below it, on the other hand, solvated proton clusters  $\text{H}^+(\text{H}_2\text{O})_n$  are the most abundant ions. An understanding of this sharp change in ionic abundance was provided by a series of elegant mass-spectroscopic studies in flowing afterglows pioneered by Ferguson and co-workers<sup>155</sup> and by a related investigation using the selected-ion flow tube (SIFT) techniques.<sup>156</sup> These revealed that in the presence of traces of water, the  $\text{O}_2^+$  readily forms the hydrated  $\text{O}_2^+(\text{H}_2\text{O})$  and  $\text{O}_2^+(\text{H}_2\text{O})_2$  clusters. Reactions with further water molecules, however, result in a switch in the ionic core



A similar sequence of reactions is also found to occur for the hydrated  $\text{NO}^+$  ions. A direct addition of water to  $\text{NO}^+$  was found to be too slow to account for its disappearance, but hydrates are formed indirectly, first by addition of, e.g., molecular nitrogen, forming an  $\text{NO}^+\text{N}_2$  ion, which then ligand-exchanges with water to form  $\text{NO}^+(\text{H}_2\text{O})$  and can then attach additional water to yield  $\text{NO}^+(\text{H}_2\text{O})_2$ . The dihydrate ion then similar to the oxygen case reacts with additional water molecules resulting again in a core switch, yielding a nitrous acid molecule and a hydrated proton

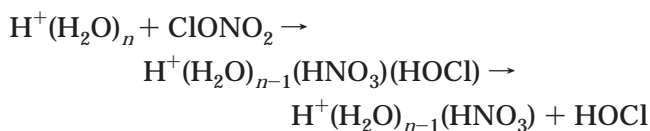


The conversion of the primary  $\text{NO}^+$  and  $\text{O}_2^+$  ions into the hydrated proton clusters requires stabilization by three-body collisions, a process which depends on the third power of pressure. It is this steep pressure dependence of the complex formation which is responsible for the relatively sharp atmospheric boundary: above about 85 km the three-body collisions are too infrequent to allow the complex stabilization. The change in the core ion could recently be beautifully confirmed by infrared-spectroscopic studies of size-

selected  $\text{NO}^+(\text{H}_2\text{O})_n$  clusters for  $n \leq 5$ , which showed clearly that above  $n = 3$  the cluster is a hydrated proton with an attached nitrous acid, HONO, molecule.<sup>157</sup> While according to some more recent studies<sup>158,159</sup> the exact number of water ligands needed for the core switch to occur is still somewhat controversial, there seems little doubt that the ionization of nitrogen oxides, hydration of the ions, and the subsequent core switch make an essential contribution to the formation of hydrated proton clusters in the upper atmosphere.

Water is also involved in another important process, a seasonal depletion of stratospheric ozone in polar latitudes, more commonly referred to as "ozone hole". The primary causes of this phenomenon are halogens of anthropogenic origin which essentially catalyze the destruction of ozone.<sup>160</sup> Halogens have long lifetimes in the stratosphere, but they are gradually converted into more stable and less chemically active forms, so-called "reservoir compounds", mainly HCl and chlorine nitrate,  $\text{ClONO}_2$ . When the polar winter temperatures drop below about  $-80^\circ\text{C}$ , the so-called polar stratospheric clouds (PSCs) may form, despite the low water content of the stratosphere. These clouds consist of microscopic  $\approx 1\text{--}10\ \mu\text{m}$  particles containing water, nitric acid, and its hydrates (NAT). The reservoir compounds HCl and  $\text{ClONO}_2$  may also condense on these particles, with heterogeneous reactions on their surface converting them back to more active species. During the polar spring, when the temperatures rise again and the PSC's evaporate, the halogens in their active form are returned to the stratosphere and produce, by their catalytic effect, the observed ozone depletion.

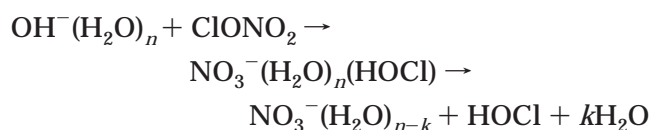
The large ionic water clusters in an FT-ICR instrument can be viewed as interesting model systems for such stratospheric processes; their reactions with both HCl<sup>40,123</sup> and  $\text{ClONO}_2$ <sup>161</sup> have recently been investigated. Chlorine nitrate was found to react rather efficiently with both anionic and cationic clusters, in each case being hydrolyzed on the cluster surface to yield nitric acid and hypochlorous acid, HOCl. In the case of the "acid",  $\text{H}^+$ -containing clusters, the efficiency was estimated to be approximately 4% of the collisional rate and the HOCl produced was found to "evaporate" almost immediately from the cluster



There was an interesting break in the distribution of the  $\text{H}^+(\text{H}_2\text{O})_m(\text{HNO}_3)$  products, with clusters with  $n \geq 6$  and  $m = 0$  being abundant, the  $m = 2$  and 3 appearing only weakly and  $m = 4$  and 5 almost completely missing. This observation is due to a change in the internal structure of the cluster and in its "ionic core". While the larger clusters are indeed hydrated protons with a "dissolved" nitric acid molecule, the very small species do not contain a proton but are better described as  $\text{NO}_2^+(\text{H}_2\text{O})_m$  with  $m =$

0–2. This is a further example of the effect of hydration: while the ionization potential of a hydrogen atom is 1312 kJ/mol, that of  $\text{NO}_2$  is only 944 kJ/mol. The presence of at least four water ligands can offset this difference and make the solvated proton more stable. This size-dependent change in internal structure could again be nicely demonstrated by infrared spectroscopy. Spectra of the size-selected hydrated  $\text{NO}_2^+(\text{H}_2\text{O})_n$  species up to  $n = 5$  confirmed that while the small  $n \leq 3$  clusters indeed have the  $\text{NO}_2^+(\text{H}_2\text{O})_n$  structure, those with  $n \geq 4$  are better described as hydrated proton clusters with a nitric acid molecule attached,  $\text{H}^+(\text{H}_2\text{O})_n(\text{HNO}_3)$ .<sup>162</sup> It would be interesting to extend the spectroscopic study to even larger-size clusters, in particular, to above  $n = 6$ , where undoubtedly ionic dissociation of the nitric acid and formation of a second proton and a nitrate anion,  $\text{NO}_3^-$ , must take place. In collisional fragmentation studies of hydrated  $\text{NO}_2^+(\text{H}_2\text{O})_n$  clusters by Stace and co-workers, both  $\text{H}_2\text{O}$  ligand loss and loss of  $\text{HNO}_3$  were observed.<sup>163</sup>

Like the cationic clusters, also the anionic, basic water clusters react rather efficiently with chlorine nitrate but with several differences. The reaction rate of the anions is about a factor of 20 higher than that of the cations and approaches the collisional rate. In addition, one observes in contrast with the protonated "acid" clusters, in particular for the larger clusters, at least transiently chlorine-containing products with appreciable intensities



In the anionic case, the HOCl is apparently bound somewhat more strongly to the "basic" cluster and is retained in about 50% of the primary product ions, but in the subsequent blackbody fragmentation, all of the hypochlorous acid is lost just as in the case of the cations.<sup>86,161</sup> The reaction mechanisms of both "acid" and "basic" cluster reactions are shown schematically in Figure 10. The weakly bound nature of HOCl and its efficient loss in collisional fragmentation was also reported in a recent study of hydrated chloride clusters,  $\text{Cl}^-(\text{H}_2\text{O})_n$ .<sup>164</sup>

Recent flow-tube studies of chlorine nitrate reactions with water ice surfaces also reported an efficient formation of gaseous HOCl and described it by a neutral mechanism.<sup>165,166</sup> It should, however, be noted that real PSCs are far from pure water, containing considerable quantities of nitric and sulfuric acid and consequently a high concentration of ionic species. The latest theoretical treatment of the problem suggested the importance of proton-transfer reactions.<sup>167–169</sup> In view of the much higher efficiency observed in the cluster studies for the "anionic",  $\text{OH}^-$ -containing clusters than for the protonated species, a "basic" reaction mechanism of Figure 10 appears perhaps more likely. The efficient formation of HOCl and its facile evaporation from the clusters may have important implications for the stratospheric reactions. It also suggests that molecular  $\text{Cl}_2$  is unlikely

**Table 3. Experimental Studies of Cationic Water Cluster Reactions. This Table Provides a List of Reactive Studies for Reference Purposes**

type of cluster	size range	reactants	major products <sup>a</sup> or dominant type of reaction	method <sup>b</sup>	ref
H <sup>+</sup> (H <sub>2</sub> O) <sub>n</sub>	1–3	H <sub>2</sub> S CH <sub>2</sub> O HCOOH CH <sub>3</sub> OH CH <sub>3</sub> CHO, C <sub>2</sub> H <sub>5</sub> OH, CH <sub>3</sub> COOH, HCOOCH <sub>3</sub> (CH <sub>3</sub> ) <sub>2</sub> O (CH <sub>3</sub> ) <sub>2</sub> CO NH <sub>3</sub>	proton transfer observed	FT	177
	1–4	CH <sub>3</sub> CN	proton transfer, ligand switching	FT	178
	~50–850	He Ar C <sub>3</sub> F <sub>8</sub> C <sub>6</sub> F <sub>6</sub>	H <sup>+</sup> (H <sub>2</sub> O) <sub>n-1</sub>	CC	179
	2–11	CH <sub>3</sub> OH NH <sub>3</sub> CH <sub>3</sub> CN CH <sub>3</sub> COCH <sub>3</sub> C <sub>5</sub> H <sub>5</sub> N	proton transfer, ligand transfer	FT	56
	1–7	CH <sub>3</sub> OH C <sub>2</sub> H <sub>5</sub> OH CH <sub>3</sub> CN furan (CH <sub>3</sub> ) <sub>2</sub> CO thiophene (C <sub>2</sub> H <sub>5</sub> ) <sub>2</sub> O pyrrole pyridine	proton transfer	HPMS	153
	3–30	CH <sub>3</sub> OH	H <sup>+</sup> (H <sub>2</sub> O) <sub>m</sub> (CH <sub>3</sub> OH) <sub>1</sub>	FT	180
	1–60	CH <sub>3</sub> CN CH <sub>3</sub> COCH <sub>3</sub> , CH <sub>3</sub> COOCH <sub>3</sub>	proton transfer, ligand switching, association	FT	181
	1–22	CH <sub>3</sub> CN	ligand switching	FT	182
	1–4	ND <sub>3</sub>	HND <sub>3</sub> <sup>+</sup> (H <sub>2</sub> O) <sub>n-2</sub>	GIB	183
	3–30	N <sub>2</sub> O <sub>5</sub>	H <sup>+</sup> (H <sub>2</sub> O) <sub>n-1</sub> (HNO <sub>3</sub> ) + HNO <sub>3</sub>	FT	50
	5–25	ClONO <sub>2</sub>	NO <sub>2</sub> <sup>+</sup> (H <sub>2</sub> O) <sub>m</sub> + (HOCl)	MB-PU	184
	2–6	Xe	H <sup>+</sup> (H <sub>2</sub> O) <sub>m</sub>	GIB	58
	n ≥ 1 <sup>c</sup>	ClONO <sub>2</sub>	NO <sub>2</sub> + (H <sub>2</sub> O) <sub>0,1</sub> , NO <sub>2</sub> + HOCl	FT	185
	1–4	isoprene diethyl ether ethanol methanol ethyl acetate acetaldehyde acetone	proton transfer	FT	186
	2–35	HCl	(H <sub>3</sub> O <sup>+</sup> ) <sub>2</sub> (Cl <sup>-</sup> )(H <sub>2</sub> O) <sub>m</sub>	ICR	40
	2–28	ClONO <sub>2</sub>	NO <sub>2</sub> <sup>+</sup> (H <sub>2</sub> O) <sub>m</sub> + HOCl	ICR	161
	3–75	(C <sub>2</sub> H <sub>5</sub> ) <sub>2</sub> O	H <sup>+</sup> (H <sub>2</sub> O) <sub>m</sub> (C <sub>2</sub> H <sub>5</sub> ) <sub>2</sub> O <sub>1</sub>	ICR	154
	2–80	(CH <sub>3</sub> ) <sub>2</sub> CO CH <sub>3</sub> CHO	ligand exchange ligand exchange, fragmentation	ICR	152
	1–3	C <sub>4</sub> H <sub>8</sub> S	proton transfer	CC	187
	1–4	(CH <sub>3</sub> ) <sub>3</sub> COH	proton transfer	IMS	188
	1–6	(CH <sub>3</sub> ) <sub>2</sub> S	ligand switching	FT	189
	1–5	(CH <sub>3</sub> ) <sub>2</sub> SO	H <sup>+</sup> (CH <sub>3</sub> SOCH <sub>3</sub> )(H <sub>2</sub> O) <sub>n-m</sub> , m = 1–4	FT	190
	1–4	OH <sup>-</sup> (H <sub>2</sub> O) <sub>1-4</sub>	H + mH <sub>2</sub> O	MB	191
D <sup>+</sup> (D <sub>2</sub> O) <sub>n</sub>	1–30	DNO <sub>3</sub>	D <sup>+</sup> (D <sub>2</sub> O) <sub>n</sub> (DNO <sub>3</sub> ), n ≥ 5	FT	192
	11–48	n HCl	D <sup>+</sup> (HCl) <sub>y</sub> (D <sub>2</sub> O) <sub>m</sub> , y = 1–4	FT	150, 151
NO <sup>+</sup> (H <sub>2</sub> O) <sub>n</sub>	0–3	H <sub>2</sub> O	H <sub>3</sub> O <sup>+</sup> (H <sub>2</sub> O) <sub>2</sub> + HNO <sub>2</sub>	FT	193
Mg <sup>+</sup> (H <sub>2</sub> O) <sub>n</sub>	17–40	HCl	MgCl <sup>+</sup> (H <sub>2</sub> O) <sub>m</sub> + H	ICR	42
MgOH <sup>+</sup> (H <sub>2</sub> O) <sub>n</sub>	9–16		MgCl <sup>+</sup> (H <sub>2</sub> O) <sub>m</sub>		
Al <sup>+</sup> (H <sub>2</sub> O) <sub>n</sub>	11–45	HCl	Al(OH)Cl <sup>+</sup> (H <sub>2</sub> O) <sub>m</sub> + H <sub>2</sub>	ICR	124
Al(OH) <sub>2</sub> <sup>+</sup> (H <sub>2</sub> O) <sub>n</sub>	7–18		Al(OH)Cl <sup>+</sup> (H <sub>2</sub> O) <sub>m</sub>		
Ag <sup>+</sup> (H <sub>2</sub> O) <sub>n</sub>	11–26	HCl	H <sub>3</sub> O <sup>+</sup> (AgCl)(H <sub>2</sub> O) <sub>m</sub>	ICR	12
Na <sup>+</sup> (H <sub>2</sub> O) <sub>n</sub>	12–28		(Na <sup>+</sup> )(Cl <sup>-</sup> )(H <sub>3</sub> O <sup>+</sup> )(H <sub>2</sub> O) <sub>m</sub>		
M <sup>2+</sup> (H <sub>2</sub> O) <sub>n</sub>	n ≤ 14	H <sub>2</sub> O, NH <sub>3</sub>	three body association	CC-ESI	146, 147

M = Be, Mg, Ca, Zn

<sup>a</sup> Product notation follows that of the original references, while it is emphasized the seeming structural implications of the given notation are not proven in all cases but sometimes only suggested. <sup>b</sup> Abbreviations are as follows: CC, collision cell; FT, flow tube; GIB, guided-ion beam; SIFT, selected-ion flow tube; TMS, tandem mass spectrometry; ICR, ion cyclotron resonance; MB, merged beams; IMS, ion mobility spectroscopy; MB-PU, molecular beam pickup. <sup>c</sup> The cluster size was not specified.



**Table 4. Experimental Studies of Anionic Water Cluster Reactions**

type of cluster	size range	reactants	major products <sup>a</sup> or dominating type of reaction	method <sup>b</sup>	ref
OH <sup>-</sup> (H <sub>2</sub> O) <sub>n</sub>	0–59	CH <sub>3</sub> CN	proton transfer and ligand switching	FT	49
O <sup>-</sup> (H <sub>2</sub> O) <sub>n</sub>			hydrogen transfer		
O <sub>2</sub> <sup>-</sup> (H <sub>2</sub> O) <sub>n</sub>			slow association		
O <sub>3</sub> <sup>-</sup> (H <sub>2</sub> O) <sub>n</sub>			slow association		
X <sup>-</sup> (H <sub>2</sub> O) <sub>n</sub> ; X = OH, O, O <sub>2</sub> H, O <sub>2</sub> , O <sub>3</sub>	0–5	N <sub>2</sub> O <sub>5</sub>	NO <sub>3</sub> <sup>-</sup> (H <sub>2</sub> O) <sub>0,1</sub>	FT	51
O <sup>-</sup> (H <sub>2</sub> O) <sub>n</sub>	0–2	O <sub>2</sub>	O <sub>3</sub> <sup>-</sup> (H <sub>2</sub> O) <sub>0,1</sub>	FT	194
		CO <sub>2</sub>	CO <sub>3</sub> <sup>-</sup>		
		CO	e <sup>-</sup>		
		NO	products		
		SO <sub>2</sub>	products		
		CH <sub>4</sub>	no reaction		
		N <sub>2</sub> O	no reaction		
		H <sub>2</sub> O	no reaction		
	0–2	H <sub>2</sub>	e <sup>-</sup> , OH <sup>-</sup> (H <sub>2</sub> O) + H	FT	195
		D <sub>2</sub>	e <sup>-</sup> , OD <sup>-</sup> (D <sub>2</sub> O) + D		
OH <sup>-</sup> (H <sub>2</sub> O) <sub>n</sub>	1–3	CO <sub>2</sub>	HOCO <sub>2</sub> <sup>-</sup> (H <sub>2</sub> O) <sub>0,1</sub>	GIB	196
	0–3	CO <sub>2</sub>	OH <sup>-</sup> (CO <sub>2</sub> )	TMS	197,198
		SO <sub>2</sub>	OH <sup>-</sup> (SO <sub>2</sub> )		
		NO <sub>2</sub>	OH <sup>-</sup> (NO <sub>2</sub> )		
	0–2	CH <sub>3</sub> Cl	Br <sup>-</sup> (H <sub>2</sub> O) <sub>0,1</sub> , Cl <sup>-</sup> (H <sub>2</sub> O) <sub>0,1</sub> + CH <sub>3</sub> OH,	TMS	199
		CH <sub>3</sub> Br	CH <sub>2</sub> Cl <sup>-</sup> , CH <sub>2</sub> Br <sup>-</sup>		
			OH <sup>-</sup> (H <sub>2</sub> O) <sub>0,1</sub>		
	0–11	HBr	Br <sup>-</sup> (H <sub>2</sub> O) <sub>m</sub>	FT	200
	0–2	ethanol	proton transfer	FT	186
		methanol			
		ethyl acetate			
		acetaldehyde			
		acetone			
O <sub>2</sub> <sup>-</sup> (H <sub>2</sub> O) <sub>n</sub>	0–4	O <sub>3</sub>	O <sub>3</sub> <sup>-</sup> (H <sub>2</sub> O) <sub>n-1</sub> + O <sub>2</sub>	FT	201
		NO	O <sub>2</sub> <sup>-</sup> (NO)(H <sub>2</sub> O) <sub>n-1</sub>		
		SO <sub>2</sub>	SO <sub>4</sub> <sup>-</sup> (H <sub>2</sub> O) <sub>m</sub>		
		CO <sub>2</sub>	CO <sub>4</sub> <sup>-</sup>		
O <sub>2</sub> H <sup>-</sup> (H <sub>2</sub> O) <sub>n</sub>	0–2	CH <sub>3</sub> CN	CH <sub>2</sub> CN <sup>-</sup> , CN <sup>-</sup>	FT	202
		CO <sub>2</sub>	HCO <sub>3</sub> <sup>-</sup> (H <sub>2</sub> O) <sub>n</sub>		
		SO <sub>2</sub>	HSO <sub>3</sub> <sup>-</sup> (H <sub>2</sub> O) <sub>n</sub> , HSO <sub>4</sub> <sup>-</sup> (H <sub>2</sub> O) <sub>n</sub>		
O <sub>2</sub> H <sup>-</sup> (CO <sub>2</sub> ) <sub>n</sub>	1	CO	no reaction	FT	203
		N <sub>2</sub> O	no reaction		
		NO	no reaction		
		NO <sub>2</sub>	no reaction		
		N <sub>2</sub> O <sub>5</sub>	NO <sub>3</sub> <sup>-</sup>		
		HNO <sub>3</sub>	NO <sub>3</sub> <sup>-</sup> , HNO <sub>2</sub> <sup>-</sup> (HNO <sub>3</sub> )		
		SO <sub>3</sub>	HSO <sub>4</sub> <sup>-</sup>		
O <sup>-</sup> (D <sub>2</sub> O) <sub>n</sub>	0–3	DNO <sub>3</sub>	NO <sub>3</sub> <sup>-</sup> (D <sub>2</sub> O) <sub>0,1</sub>	FT	204
OD <sup>-</sup> (D <sub>2</sub> O) <sub>n</sub>			NO <sub>3</sub> <sup>-</sup> (D <sub>2</sub> O) <sub>0,1</sub>		
O <sub>2</sub> <sup>-</sup> (D <sub>2</sub> O) <sub>n</sub>			NO <sub>3</sub> <sup>-</sup> (D <sub>2</sub> O) <sub>0,1</sub> , (O <sub>2</sub> DNO <sub>3</sub> ) <sup>-</sup>		
DO <sub>2</sub> <sup>-</sup> (D <sub>2</sub> O) <sub>n</sub>			NO <sub>3</sub> <sup>-</sup> (D <sub>2</sub> O) <sub>0,1</sub> , (DO <sub>2</sub> DNO <sub>3</sub> ) <sup>-</sup>		
O <sub>3</sub> <sup>-</sup> (D <sub>2</sub> O) <sub>n</sub>			NO <sub>3</sub> <sup>-</sup> (D <sub>2</sub> O) <sub>0,1</sub>		
O <sup>-</sup> (D <sub>2</sub> O) <sub>n</sub>	0–5	NO	NO <sub>2</sub> <sup>-</sup> (D <sub>2</sub> O) <sub>m</sub>	FT	205
OD <sup>-</sup> (D <sub>2</sub> O) <sub>n</sub>			no reactions		
O <sub>2</sub> <sup>-</sup> (D <sub>2</sub> O) <sub>n</sub>			OONO <sup>-</sup> (D <sub>2</sub> O) <sub>m</sub>		
DO <sub>2</sub> <sup>-</sup> (D <sub>2</sub> O) <sub>n</sub>			NO <sub>2</sub> <sup>-</sup> (D <sub>2</sub> O) <sub>m</sub> + OD		
X <sup>-</sup> (D <sub>2</sub> O) <sub>n</sub> ; X = O, OD, O <sub>2</sub> , DO <sub>2</sub> , O <sub>3</sub>	0–4	Cl <sub>2</sub> O	Cl <sup>-</sup> (DOCl), ClO <sup>-</sup> (DOCl)	FT	206
NO <sub>2</sub> <sup>-</sup> (H <sub>2</sub> O) <sub>n</sub>	0–2	N <sub>2</sub> O <sub>5</sub>	NO <sub>3</sub> <sup>-</sup> , (NO <sub>3</sub> HNO <sub>3</sub> ) <sup>-</sup>	FT	207
NO <sub>3</sub> <sup>-</sup> (H <sub>2</sub> O) <sub>n</sub>	1, 2		(NO <sub>3</sub> HNO <sub>3</sub> ) <sup>-</sup>		
NO <sub>2</sub> <sup>-</sup> (D <sub>2</sub> O) <sub>n</sub>	0–2	Cl <sub>2</sub> O	NO <sup>-</sup> (D <sub>2</sub> O) <sub>0,1</sub> , (Cl <sub>2</sub> ONO <sub>2</sub> ) <sup>-</sup>	FT	208
NO <sub>3</sub> <sup>-</sup> (D <sub>2</sub> O) <sub>n</sub>	0–2		Cl <sub>2</sub> O <sup>-</sup>		
Cl <sup>-</sup> (D <sub>2</sub> O) <sub>n</sub>	0–2		Cl <sub>3</sub> <sup>-</sup> , Cl <sub>3</sub> O <sup>-</sup>		
Cl <sup>-</sup> (D <sub>2</sub> O) <sub>n</sub>	0–3	ClONO <sub>2</sub>	NO <sub>3</sub> <sup>-</sup> (D <sub>2</sub> O) <sub>n-1</sub>	FT	164
(HO) <sub>2</sub> PO <sub>2</sub> <sup>-</sup> (H <sub>2</sub> O) <sub>n</sub>	0–2	Ar, Δ	PO <sub>3</sub> <sup>-</sup> + H <sub>2</sub> O (n = 1 only)	CC	209
		H <sub>2</sub> O	(HO) <sub>2</sub> PO <sub>2</sub> <sup>-</sup> (H <sub>2</sub> O) <sub>n+1</sub>	210	
OH <sup>-</sup> (H <sub>2</sub> O) <sub>n</sub>	1–50	HCl	Cl <sup>-</sup> (H <sub>2</sub> O) <sub>n-2</sub>	ICR	123
O <sup>-</sup> (H <sub>2</sub> O) <sub>n</sub>			Cl <sup>-</sup> (H <sub>2</sub> O) <sub>m</sub> + OH, ClHO <sup>-</sup> (H <sub>2</sub> O) <sub>n</sub>		
X <sup>-</sup> (H <sub>2</sub> O) <sub>n</sub> ; X = OH, O	2–100	ClONO <sub>2</sub>	NO <sub>3</sub> <sup>-</sup> (H <sub>2</sub> O) <sub>m</sub> , NO <sub>3</sub> <sup>-</sup> (HOCl)(H <sub>2</sub> O) <sub>m</sub>	ICR	161
OH <sup>-</sup> (H <sub>2</sub> O) <sub>n</sub>	2–30	CH <sub>3</sub> CHO	(CH <sub>3</sub> COO <sup>-</sup> (H <sub>2</sub> O) <sub>m</sub> + H,	ICR	152
O <sup>-</sup> (H <sub>2</sub> O) <sub>n</sub>			CH <sub>2</sub> CHO <sup>-</sup> (H <sub>2</sub> O) <sub>m</sub>		
O <sub>2</sub> <sup>-</sup> (H <sub>2</sub> O) <sub>n</sub>	1–33	hν	O <sub>2</sub> <sup>-</sup> (H <sub>2</sub> O) <sub>n-m</sub> , O <sup>-</sup> (H <sub>2</sub> O) <sub>n</sub>	TMS	211
F <sup>-</sup> (H <sub>2</sub> O) <sub>n</sub>	0–5	CH <sub>3</sub> Br	Br <sup>-</sup> (H <sub>2</sub> O) <sub>0,1</sub>	FT	212
			F <sup>-</sup> (H <sub>2</sub> O) <sub>2</sub> (CH <sub>3</sub> Br)		
			F <sup>-</sup> (H <sub>2</sub> O) <sub>3,4</sub>		

Table 4 (Continued)

type of cluster	size range	reactants	major products <sup>a</sup> or dominating type of reaction	method <sup>b</sup>	ref
F <sup>-</sup> (D <sub>2</sub> O) <sub>n</sub>	0–6	Cl <sub>2</sub>	Cl <sup>-</sup> , FCl <sub>2</sub> <sup>-</sup> (D <sub>2</sub> O) <sub>m</sub> + (n – m)D <sub>2</sub> O; m < n	FT	213
Cl <sup>-</sup> (D <sub>2</sub> O) <sub>n</sub>	0–8		Cl <sup>-</sup> , Cl <sub>3</sub> <sup>-</sup> (D <sub>2</sub> O) <sub>m</sub> + (n – m)D <sub>2</sub> O; m < n		
Br <sup>-</sup> (D <sub>2</sub> O) <sub>n</sub>	0–16		Cl <sup>-</sup> , BrCl <sub>2</sub> <sup>-</sup> (D <sub>2</sub> O) <sub>m</sub> + (n – m)D <sub>2</sub> O; m < n		
I <sup>-</sup> (D <sub>2</sub> O) <sub>n</sub>	0–13		Cl <sup>-</sup> , ICl <sub>2</sub> <sup>-</sup> (D <sub>2</sub> O) <sub>m</sub> + (n – m)D <sub>2</sub> O; m < n		
I <sup>-</sup> (H <sub>2</sub> O) <sub>n</sub>	1–25	HCl	I <sup>-</sup> (H <sub>2</sub> O) <sub>m</sub> (HCl)	ICR	126
Cl <sup>-</sup> (H <sub>2</sub> O) <sub>n</sub>	0–5	N <sub>2</sub> O <sub>5</sub>	NO <sub>3</sub> <sup>-</sup> (H <sub>2</sub> O) <sub>m</sub> + ClONO	ICR	214
Br <sup>-</sup> (H <sub>2</sub> O) <sub>n</sub>	0–5		NO <sub>3</sub> <sup>-</sup> (H <sub>2</sub> O) <sub>m</sub> + BrONO		
(H <sub>2</sub> O) <sub>n</sub> <sup>-</sup>	15–30	O <sub>2</sub>	O <sub>2</sub> <sup>-</sup> (H <sub>2</sub> O) <sub>n-7</sub>	MB–PU	171
CO <sub>2</sub>	CO <sub>2</sub> <sup>-</sup> (H <sub>2</sub> O) <sub>n-3</sub>				
NO	NO <sup>-</sup> (H <sub>2</sub> O) <sub>n-5</sub>				
N <sub>2</sub> O	O <sup>-</sup> (H <sub>2</sub> O) <sub>n-5</sub> + N <sub>2</sub>				
Br <sub>2</sub>	Br <sup>-</sup> (H <sub>2</sub> O) <sub>n-5</sub> + Br				
CH <sub>3</sub> Br	Br <sup>-</sup> (H <sub>2</sub> O) <sub>n-4</sub> + CH <sub>3</sub>				
(H <sub>2</sub> O) <sub>n</sub> <sup>-</sup>	6–25	D <sub>2</sub> O	D <sub>2</sub> O(H <sub>2</sub> O) <sub>n-1</sub> <sup>-</sup> + H <sub>2</sub> O	MB–PU	170

<sup>a</sup> Product notation follows that of the original references, while it is emphasized the seeming structural implications of the given notation are not proven in some cases but sometimes only suggested. <sup>b</sup> Abbreviations are as follows: CC, collision cell; FT, flow tube; GIB, guided-ion beam; SIFT, selected-ion flow tube; TMS, tandem mass spectrometry; ICR, ion cyclotron resonance; MB, merged beams; IMS, ion mobility spectroscopy; MB–PU, molecular-beam pickup up.

to be formed directly but more probably in a two-step process involving HOCl intermediates.

### G. Selected other Reactions of Water Clusters and Hydrated Ions

The few topics on which we concentrated on the previous pages are naturally far from comprehensively covering the available literature on water clusters and their reactions. The research in this area is so extensive that an exhaustive review would require several volumes. As already noted in the Introduction, we have therefore attempted to focus our discussion mainly on studies of the ionic water clusters using the FT-ICR technique, which is also central to the work done in our own laboratory, and addressed other areas more superficially when needed for comparison or when appropriate to clarify some point. Even the discussion of ionic water clusters is not exhaustive, but we have tried to focus on those clusters which we judged of particular interest and which have not recently been reviewed elsewhere. In Tables 3 and 4 we list, in addition to the reactions explicitly discussed in this review, a variety of other previously reported reactions of hydrated ion clusters with both organic and inorganic compounds.

We have already mentioned superficially solvated electrons, e<sup>-</sup>(H<sub>2</sub>O)<sub>n</sub>, which are a fascinating topic and where there is now extensive literature on experimental and theoretical studies in this area by Johnson, Bowen, and other investigators.<sup>19,79,80,167</sup> While the laser vaporization source of the type used in our laboratory only produces large species (n > 20), with special care much smaller clusters can be generated also. The fact that besides the presumably dipole-bound dimer anion, n = 2, the smallest negative water cluster observed is the hexamer may reflect the fact that n = 6 is believed to be the smallest cluster with a truly three-dimensional structure, since the n = 3, 4, and 5 neutral species exhibit nearly planar ring geometries. The hydrated electron clusters exhibit numerous interesting reactions: they easily transfer the extra electron to molecules with a higher electron affinity and undergo a variety of ligand-exchange reactions. They can also attach an

additional ligand with simultaneous detachment of the electron.<sup>170,171</sup> There is also a wide range of interesting areas worthy of further study. Quite interesting are the effects of a blackbody radiation on the solvated electron clusters and the competition between fragmentation and electron detachment. In any event, solvated electron clusters are one example of a subject which was previously reviewed, but when considering the activity in this field, a new review would probably not be out of place.

As already mentioned, discharge sources also yield, besides clusters containing OH<sup>-</sup>(H<sub>2</sub>O)<sub>n</sub>, smaller quantities of other ions with usually hydrated O<sup>-</sup> clusters ranking second in abundance. These open-shell ions are also of considerable interest and seem to be much more reactive than the OH<sup>-</sup> species; for instance, they seem to react with acetaldehyde about an order of magnitude more efficiently than the hydroxyl-containing ion and presumably oxidize it to acetate.<sup>152</sup> As a possible explanation for the reactivity difference, it was suggested that while the OH<sup>-</sup>, which may form a hydrogen bond, is solvated internally, the O<sup>-</sup> anion may reside on the surface of the clusters.

### V. Summary

While bulk water and pure neutral water clusters have been extensively studied, water containing impurity molecules or ions is at least an equally important topic. In general, the properties of water are drastically modified by impurities: impurity ions give it its electric conductivity and other properties, control its acidity and pH value, and have a decisive effect upon its chemical reactivity. The very importance of water as an industrial solvent, on the one hand, and as a cause of corrosion, on the other, implies the importance of “impure” water. Similarly, while water is the solvent of life, from a biological point of view living organisms could not survive in pure water. This importance of aqueous solutions and molecule and ion hydration provide one of the motivations for studying ionic water clusters and hydrated ions.

Ion sources, in particular sources combining pulsed supersonic expansion with laser vaporization, permit

the production of hydrated ions of the type  $X^{\pm}(H_2O)_n$ , where X can be an anion or cation of essentially any atom or of a simple molecule and the number of ligands can easily range up to  $\approx 200$ . Such hydrated clusters, when trapped in high vacuum of an FT-ICR mass spectrometer, gradually fragment due to absorption of the blackbody radiation from the apparatus walls. The blackbody fragmentation provides a simple way of gently removing the solvent molecules one by one and observing its effect upon the ion stability and reactions occurring in the cluster.

Clusters containing protons,  $H^+$ , on the one hand, or  $OH^-$ , on the other, are in many respects found to behave as an acid or basic aqueous medium, respectively. These ionic water clusters thus provide an interesting medium, in which a wide range of substances can be dissolved, and numerous solution processes such as ionic dissolution, ion recombination, neutralization or precipitation reactions, proton transfer, as well as reduction-oxidation reactions can be investigated in microscopic detail. The water clusters can also "dissolve" numerous organic compounds and can be used as a medium for studies of aqueous organic reactions.

Many important atmospheric processes are at least in part due to heterogeneous reactions occurring on the surface of atmospheric aerosols and droplets or to reactions of hydrated ions. Some examples are smog formation, the seasonal stratospheric ozone depletion on polar stratospheric clouds, or formation of halogens from marine aerosols. Hydrated clusters of a suitable composition can thus provide simplified model systems for convenient laboratory studies of these processes. Thus, catalytic decomposition of chlorine nitrate on the water cluster surface or reactions of hydrochloric acid with ionic water clusters represent some examples recently studied.

Coupling of tunable lasers to ICR-MS instruments permits a convenient and direct means for studies of spectroscopy of ionic water clusters and solvated ions via their photofragmentation or fluorescence. The few studies reported in this area have already yielded interesting information about cluster stabilities and internal structures and provide bright perspectives for future investigations in this direction.

The blackbody fragmentation itself gives interesting qualitative information about cluster stability and indirectly can yield some insight into their structure. The use of ICR cells with heated walls extends the usefulness of this method to studying the stability of more strongly bound species and permits via temperature dependence more quantitative determinations of the binding energies. Similar experiments with cooled cells should in the future permit extension of such investigations in the opposite direction to more weakly bound species and hydrates. It should also make a much wider range of water cluster sizes amenable to experimental study and allow easier control of the cluster internal temperature. Combined with electrospray sources, a variety of biological systems can be studied also, and an apparatus designed for this purpose in our laboratory is currently being completed.

## VI. References

- (1) Huisken, F. *Adv. Chem. Phys.* **1992**, *81*, 63–140.
- (2) Buck, U. *Springer Ser. Chem. Phys.* **1994**, *52*, 396–418.
- (3) *Structure and Reactivity in Aqueous Solutions*; Cramer, C. J., Truhlar, D. G., Eds.; American Chemical Society: Washington, D.C., 1994; Vol. 568.
- (4) Liu, K.; Cruzan, J. D.; Saykally, R. J. *Science* **1996**, *271*, 929–33.
- (5) NATO Advanced Study Institute on Recent Theoretical and Experimental Advances in Hydrogen-Bonded Clusters, Elounda, Crete, Greece, 1997.
- (6) Buck, U. *Adv. Mol. Vib. Collision Dyn.* **1998**, *3*, 127–161.
- (7) International Conference on Water in the Gas Phase, Marne la Vallée, Paris, France, 1998.
- (8) 218th National ACS Meeting with Symposium on Water and Water Clusters, New Orleans, LA, 1999.
- (9) Lehninger, A. L.; Nelson, D. L.; Cox, M. M. *Principles of Biochemistry*, 2nd ed.; Worth Publishers: New York, 1993.
- (10) Searcy, J. Q.; Fenn, J. B. *J. Chem. Phys.* **1974**, *61*, 5282–5288.
- (11) Beyer, M.; Berg, C.; Goerlitz, H.; Schindler, T.; Achatz, U.; Niedner-Schatteburg, G.; Bondybey, V. E. *J. Am. Chem. Soc.* **1996**, *118*, 7386–7389.
- (12) Fox, B. S.; Beyer, M. K.; Achatz, U.; Joos, S.; Niedner-Schatteburg, G.; Bondybey, V. E. *J. Phys. Chem.* **2000**, *104*, 1147–1151.
- (13) Rodriguez-Cruz, S. E.; Klassen, J. S.; Williams, E. R. *J. Am. Soc. Mass Spectrom.* **1997**, *8*, 565–568.
- (14) Märk, T. D.; Castleman, A. W., Jr. *Adv. At. Mol. Phys.* **1984**, *20*, 65–172.
- (15) Castleman, A. W., Jr.; Wei, S. *Annu. Rev. Phys. Chem.* **1994**, *45*, 685–719.
- (16) Castleman, A. W., Jr. *Adv. Gas-Phase Ion Chem.* **1998**, *3*, 185–253.
- (17) Fuke, K.; Hashimoto, K.; Iwata, S. In *Advances in Chemical Physics*; John Wiley & Sons: New York, 1999; Vol. 110.
- (18) De Haan, D. O.; Brauers, T.; Oum, K.; Stutz, J.; Nordmeyer, T.; Finlayson-Pitts, B. J. *Int. Rev. Phys. Chem.* **1999**, *18*, 343–385.
- (19) Armbruster, M.; Haberland, H.; Schindler, H.-G. *Phys. Rev. Lett.* **1981**, *47*, 323.
- (20) Scoles, G. *Atomic and Molecular Beam Methods*; Oxford University Press: New York and Oxford, 1988.
- (21) Haberland, H. In *Clusters of Atoms and Molecules*; Haberland, H., Ed.; Springer-Verlag: Berlin, 1994; Vol. I.
- (22) Yamashita, M.; Fenn, J. B. *J. Phys. Chem.* **1984**, *88*, 4451.
- (23) Yamashita, M.; Fenn, J. B. *J. Phys. Chem.* **1984**, *88*, 4671.
- (24) *Electrospray Ionization Mass Spectrometry: Fundamentals, Instrumentation & Applications*; Cole, R. B., Ed.; John Wiley & Sons Inc.: New York, 1997.
- (25) Klassen, J. S.; Ho, Y.; Blades, A. T.; Kebarle, P. *Adv. Gas-Phase Ion Chem.* **1998**, *3*, 255–318.
- (26) Rodriguez-Cruz, S. E.; Jockusch, R. A.; Williams, E. R. *J. Am. Chem. Soc.* **1998**, *120*, 5842–5843.
- (27) Rodriguez-Cruz, S. E.; Jockusch, R. A.; Williams, E. R. *J. Am. Chem. Soc.* **1999**, *121*, 1986–1987.
- (28) Fenn, J. B.; Mann, M.; Meng, C. K.; Wong, S. F.; Whitehouse, C. M. *Science* **1989**, *246*, 64–71.
- (29) Loscertales, I. G.; Mora, F. d. I. *J. Chem. Phys.* **1995**, *103*, 5041–3060.
- (30) Kebarle, P. *J. Mass Spectrom.* **1997**, *32*, 922–929.
- (31) Satkiewicz, F. G.; Myer, J. A.; Warneck, P. *Techniques Applicable to Mass Spectrometry of Gaseous Trace Contaminants*; GCA Corp., 1969.
- (32) Lancaster, G. M.; Honda, F.; Fukuda, Y.; Rabalais, J. W. *J. Am. Chem. Soc.* **1979**, *101*, 1951–1958.
- (33) Magnera, T. F.; David, D. E.; Michl, J. *Chem. Phys. Lett.* **1991**, *182*, 363.
- (34) Magnera, T. F.; David, D. E.; Michl, J. *J. Am. Chem. Soc.* **1989**, *111*, 4100.
- (35) Magnera, T. F.; David, D. E.; Stulik, D.; Orth, R. G.; Jonkman, H. T.; Michl, J. *J. Am. Chem. Soc.* **1989**, *111*, 5036.
- (36) Bassi, D. In *Atomic and Molecular Beam Methods*; Scoles, G., Ed.; Oxford University Press: New York, Oxford, 1988; Vol. I.
- (37) Engelking, P. C. *Rev. Sci. Instrum.* **1986**, *57*, 2274.
- (38) Bondybey, V. E.; English, J. H. *J. Chem. Phys.* **1981**, *74*, 6978–9.
- (39) Dietz, T. G.; Duncan, M. A.; Powers, D. E.; Smalley, R. E. *J. Chem. Phys.* **1981**, *74*, 6511.
- (40) Schindler, T.; Berg, C.; Niedner-Schatteburg, G.; Bondybey, V. E. *Chem. Phys. Lett.* **1994**, *229*, 57–64.
- (41) Berg, C.; Achatz, U.; Beyer, M.; Joos, S.; Albert, G.; Schindler, T.; Niedner-Schatteburg, G.; Bondybey, V. E. *Int. J. Mass Spectrom. Ion Processes* **1997**, *167*, 723–734.
- (42) Berg, C.; Beyer, M.; Achatz, U.; Niedner-Schatteburg, G.; Bondybey, V. E. *Chem. Phys.* **1998**, *239*, 379–392.
- (43) Kebarle, P. In *Techniques for the study of ion-molecule reactions*; Farrar, J. M., Saunders, W. H., Jr., Eds.; John Wiley & Sons: New York, 1988.
- (44) Kebarle, P.; Hogg, A. M. *J. Chem. Phys.* **1965**, *42*, 798.



- (45) Fehsenfeld, F. C.; Ferguson, E. E.; Schmeltekopf, A. L. *J. Chem. Phys.* **1966**, *44*, 3022–3024.
- (46) Ferguson, E. E.; Fehsenfeld, F. C.; Schmeltekopf, A. L. *Adv. At. Mol. Phys.* **1969**, *5*, 1–56.
- (47) Good, A.; Durden, D. A.; Kebarle, P. *J. Chem. Phys.* **1970**, *52*, 212.
- (48) Good, A.; Durden, D. A.; Kebarle, P. *J. Chem. Phys.* **1970**, *52*, 222.
- (49) Yang, X.; Zhang, X.; Castleman, A. W., Jr. *J. Phys. Chem.* **1991**, *95*, 8520–8524.
- (50) Wincel, H.; Mereand, E.; Castleman, A. W., Jr. *J. Phys. Chem.* **1994**, *98*, 8606–8610.
- (51) Wincel, H.; Mereand, E.; Castleman, A. W., Jr. *J. Phys. Chem.* **1995**, *99*, 1792–8.
- (52) Arshadi, M.; Yamadagni, R.; Kebarle, P. *J. Phys. Chem.* **1970**, *74*, 1475.
- (53) Hiraoka, K.; Misuzu, S.; Yamabe, S. *J. Phys. Chem.* **1988**, *92*, 3943–3952.
- (54) Keesee, R. G.; Castleman, A. W., Jr. *J. Phys. Chem. Ref. Data* **1986**, *15*, 1011–1071.
- (55) Kebarle, P.; Searles, S. K.; Zolla, A.; Scarborough, J.; Arshadi, M. *J. Am. Chem. Soc.* **1967**, *89*, 6393.
- (56) Viggiano, A. A.; Dale, F.; Paulson, J. F. *J. Chem. Phys.* **1988**, *88*, 2469–2477.
- (57) Gerlich, D. In *State-Selected and State-to-State Ion-Molecule Reaction Dynamics, Part 1. Experiments*; Baer, M., Ng, C.-Y., Eds.; John Wiley & Sons: New York, 1992; Vol. LXXXI.
- (58) Dalleska, N. F.; Honma, K.; Armentrout, P. B. *J. Am. Chem. Soc.* **1993**, *115*, 12125–31.
- (59) Gentry, W. R. In *Gas-Phase Ion Chemistry*; Bowers, M. T., Ed.; Academic Press: New York, 1979; Vol. 2.
- (60) *Techniques for the study of ion-molecule reactions*; Farrar, J. M., Saunders, W. H. J., Eds.; John Wiley & Sons: New York, 1988; Vol. XX.
- (61) Marshall, A. G.; Verdun, F. R. *Fourier Transforms in NMR, Optical, and Mass Spectrometry*; Elsevier: Amsterdam, 1990.
- (62) *FT-ICR/MS: Analytical Applications of Fourier Transform Ion Cyclotron Resonance Mass Spectrometry*; Asamoto, B., Ed.; VCH Publisher Inc.: New York, Weinheim, Cambridge, 1991.
- (63) Beuhler, R. J.; Friedlander, G.; Friedman, L. *Phys. Rev. Lett.* **1989**, *63*, 1292.
- (64) Klassen, J. S.; Blades, A. T.; Kebarle, P. *J. Phys. Chem.* **1995**, *99*, 15509–17.
- (65) Blades, A. T.; Klassen, J. S.; Kebarle, P. *J. Am. Chem. Soc.* **1995**, *117*, 10563–71.
- (66) Meot-Ner, M. *J. Am. Chem. Soc.* **1992**, *114*, 3312–22.
- (67) El-Shall, M. S.; Daly, G. M.; Gao, J.; Meot-Ner, M.; Sieck, L. W. *J. Phys. Chem.* **1992**, *96*, 507–10.
- (68) Kebarle, P. In *Modern Aspects of Electrochemistry*; Conway, B. E., Bockris, J. O. M., Eds.; Plenum Press: New York, 1974; Vol. 9.
- (69) Keesee, R. G.; Lee, N.; Castleman, A. W., Jr. *J. Chem. Phys.* **1980**, *73*, 2195–2202.
- (70) Keesee, R. G.; Castleman, A. W., Jr. *Chem. Phys. Lett.* **1980**, *74*, 139–142.
- (71) Lee, N.; Keesee, R. G.; Castleman, A. W., Jr. *J. Colloid Interface Sci.* **1980**, *75*, 555.
- (72) Tissandier, M. D.; Cowen, K. A.; Feng, W. Y.; Gundlach, E.; Cohen, M. H.; Earhart, A. D.; Coe, J. V.; Tuttle, T. R., Jr. *J. Phys. Chem. A* **1998**, *102*, 7787–7794.
- (73) Tawa, G. J.; Topol, I. A.; Burt, S. K.; Caldwell, R. A.; Rashin, A. A. *J. Chem. Phys.* **1998**, *109*, 4852–4863.
- (74) Bockris, J. O. M.; Reddy, A. K. N. *Modern Electrochemistry*; Plenum Press: New York, 1970.
- (75) Coe, J. V.; Earhart, A. D.; Cohen, M. H.; Hoffman, G. J.; Sarkas, H. W.; Bowen, K. H. *J. Chem. Phys.* **1997**, *107*, 6023–6031.
- (76) Lifshitz, C. In *Cluster Ions*; Ng, C. Y., Baer, T., Powis, I., Eds.; Wiley: Chichester, 1993.
- (77) Gotts, N. G.; Lethbridge, P. G.; Stace, A. J. *J. Chem. Phys.* **1992**, *96*, 408–21.
- (78) Shinohara, H.; Nishi, N.; Washida, N. *J. Chem. Phys.* **1986**, *84*, 5561–5567.
- (79) Campagnola, P. J.; Posey, L. A.; Johnson, M. A. *J. Chem. Phys.* **1991**, *95*, 7998–8004.
- (80) Ayotte, P.; Bailey, C. G.; Kim, J.; Johnson, M. A. *J. Chem. Phys.* **1998**, *108*, 444–449.
- (81) Zwier, T. S. In *Molecular Clusters*; Bowmann, J. M., Bacic, Z., Eds.; JAI Press Inc.: Stamford, CT, 1998; Vol. 3.
- (82) Thorne, L. R.; Beauchamp, J. L. In *Gas-Phase Ion Chemistry*; Bowers, M. T., Ed.; Academic Press: Orlando, 1984; Vol. 3.
- (83) Castleman, A. W. J.; Bowen, K. H., Jr. *J. Phys. Chem.* **1996**, *100*, 12911–12944.
- (84) Albert, G.; Berg, C.; Beyer, M.; Achatz, U.; Joos, S.; Niedner-Schatteburg, G.; Bondybey, V. E. *Chem. Phys. Lett.* **1997**, *268*, 235–241.
- (85) Beyer, M.; Berg, C.; Albert, G.; Achatz, U.; Bondybey, V. E. *Chem. Phys. Lett.* **1997**, *280*, 459–463.
- (86) Schindler, T.; Berg, C.; Niedner-Schatteburg, G.; Bondybey, V. E. *Chem. Phys. Lett.* **1996**, *250*, 301–8.
- (87) Beyer, M.; Berg, C.; Albert, G.; Achatz, U.; Joos, S.; Niedner-Schatteburg, G.; Bondybey, V. E. *J. Am. Chem. Soc.* **1997**, *119*, 1466–1467.
- (88) Fox, B. S.; Joos, S.; Achatz, U.; Niedner-Schatteburg, G.; Bondybey, V. E. Manuscript in preparation.
- (89) Thoelmann, D.; Tonner, D. S.; McMahon, T. B. *J. Phys. Chem.* **1994**, *98*, 2002–4.
- (90) Dunbar, R. C.; McMahon, T. B.; Thölmann, D.; Tonner, D. S.; Salahub, D. R.; Wei, D. *J. Am. Chem. Soc.* **1995**, *117*, 12819–12825.
- (91) Perrin, J. Gallimard, Paris, reprint 1970.
- (92) Langmuir, I. *J. Am. Chem. Soc.* **1920**, *42*, 2190–2205.
- (93) Lindemann, F. A. *Trans. Faraday Soc.* **1922**, *17*, 598.
- (94) Hinshelwood, C. N. *Proc. R. Soc. (A)* **1927**, *113*, 230.
- (95) Baldeschwieler, D.; Pimentel, G. C. *J. Chem. Phys.* **1960**, *33*, 1008.
- (96) Rasanen, M.; Bondybey, V. E. *Chem. Phys. Lett.* **1984**, *111*, 515.
- (97) Beyer, M.; Savchenko, E. V.; Niedner-Schatteburg, G.; Bondybey, V. E. *Low Temp. Phys.* **1999**, *25*, 814.
- (98) Tonner, D. S.; Thoelmann, D.; McMahon, T. B. *Chem. Phys. Lett.* **1995**, *233*, 324–30.
- (99) Eigen, M. *Angew. Chem.* **1963**, *75*, 489.
- (100) Eigen, M. *Angew. Chem., Int. Ed.* **1964**, *3*, 1.
- (101) Lin, S.-S. *Rev. Sci. Instrum.* **1973**, *44*, 516.
- (102) Haberland, H. In *Electronic and Atomic Collisions*; Eichler, J., Hertel, I. V., Stolterforth, N., Eds.; Elsevier: New York, 1984.
- (103) Burke, R. R.; Wayne, R. P. *Int. J. Mass Spectrom. Ion Processes* **1977**, *25*, 199.
- (104) Dreyfuss, D.; Wachman, H. Y. *J. Chem. Phys.* **1982**, *76*, 2031–2042.
- (105) Stace, A. J.; Moore, C. *Chem. Phys. Lett.* **1983**, *96*, 80–84.
- (106) Beuhler, R. J.; Friedman, L. *J. Chem. Phys.* **1982**, *77*, 2549–2557.
- (107) Shinohara, H.; Nagashima, U.; Tanaka, H.; Nishi, N. *J. Chem. Phys.* **1985**, *83*, 4183–4192.
- (108) Nagashima, U.; Shinohara, H.; Nishi, N.; Tanaka, H. *J. Chem. Phys.* **1986**, *84*, 209–214.
- (109) Echt, O.; Kreisler, D.; Knapp, M.; Recknagel, E. *Chem. Phys. Lett.* **1984**, *108*, 401–407.
- (110) Wei, S.; Shi, Z.; Castleman, A. W., Jr. *J. Chem. Phys.* **1991**, *94*, 3268–70.
- (111) Shi, Z.; Wei, S.; Ford, J. V.; Castleman, A. W., Jr. *Chem. Phys. Lett.* **1992**, *200*, 142.
- (112) Yang, X.; Castleman, A. W., Jr. *J. Phys. Chem.* **1990**, *94*, 8500–2.
- (113) Yang, X.; Castleman, A. W., Jr. *J. Phys. Chem.* **1990**, *94*, 8974.
- (114) Selinger, A.; Castleman, A. W., Jr. *J. Phys. Chem.* **1991**, *95*, 8442–4.
- (115) Selinger, A.; Castleman, A. W., Jr. *NATO ASI Ser., Ser. C* **1992**, *374*, 1137–40.
- (116) Steel, E. A.; Merz, K. M., Jr.; Selinger, A.; Castleman, A. W., Jr. *J. Phys. Chem.* **1995**, *99*, 7829–36.
- (117) Davidson, D. W. In *Water in Crystalline Hydrates, Aqueous Solutions of Simple Nonelectrolytes*; Franks, F., Ed.; Plenum Press: New York, London, 1973; Vol. II.
- (118) Berez, E.; Balla-Achs, M. *Gas Hydrates*; Elsevier: Amsterdam, 1983.
- (119) *Proceedings of the International Conference on Natural Gas Hydrates*; Sloan, E. D., Happel, J., Hnatow, M. A., Eds.; New York, 1994; Vol. 715.
- (120) Laasonen, K.; Klein, M. L. *J. Phys. Chem.* **1994**, *98*, 10079–10083.
- (121) Bondybey, V. E.; Schindler, T.; Berg, C.; Beyer, M.; Achatz, U.; Joos, S.; Niedner-Schatteburg, G. In *Hydrogen bonding in clusters*; Xantheas, S., Ed.; Kluwer Academic Publishers: Dordrecht, 2000.
- (122) Lee, S. W.; Freivogel, P.; Schindler, T.; Beauchamp, J. L. *J. Am. Chem. Soc.* **1998**, *120*, 11758.
- (123) Schindler, T.; Berg, C.; Niedner-Schatteburg, G.; Bondybey, V. E. *J. Phys. Chem.* **1995**, *99*, 12434–43.
- (124) Beyer, M.; Achatz, U.; Berg, C.; Joos, S.; Niedner-Schatteburg, G.; Bondybey, V. E. *J. Phys. Chem.* **1999**, *103*, 671–678.
- (125) Achatz, U.; Fox, B.; Joos, S.; Niedner-Schatteburg, G.; Bondybey, V. E. Manuscript in preparation.
- (126) Achatz, U.; Joos, S.; Berg, C.; Beyer, M.; Niedner-Schatteburg, G.; Bondybey, V. E. *Chem. Phys. Lett.* **1998**, *291*, 459–464.
- (127) Zundel, G. In *The Hydrogen Bond, Recent Developments in Theory and Experiments*; Schuster, P., Zundel, G., Sandorfy, C., Eds.; North-Holland: Amsterdam, 1976.
- (128) Valeev, E. F.; Schaefer, H. F., III *J. Chem. Phys.* **1998**, *108*, 7197–7201.
- (129) Tuckerman, M.; Laasonen, K.; Sprik, M.; Parrinello, M. *J. Chem. Phys.* **1995**, *103*, 150–161.
- (130) Lobaugh, J.; Voth, G. A. *J. Chem. Phys.* **1996**, *104*, 2056–2069.
- (131) Vuilleumier, R.; Borgis, D. *J. Phys. Chem. B* **1998**, *102*, 4261.
- (132) Vuilleumier, R.; Borgis, D. *J. Chem. Phys.* **1999**, *111*, 4251–4266.
- (133) Tuckerman, M. E.; Laasonen, K.; Sprik, M.; Parrinello, M. *J. Phys.: Condens. Matter* **1994**, *6*, A93–A100.

- (134) Corongiu, G.; Kelterbaum, R.; Kochanski, E. *J. Phys. Chem.* **1995**, *99*, 8038–44.
- (135) Hodges, M. P.; Stone, A. J. *J. Chem. Phys.* **1999**, *110*, 6766–6772.
- (136) Novakovskaya, Y. V.; Stepanov, N. F. *J. Phys. Chem. A* **1999**, *103*, 3285–3288.
- (137) Wei, D.; Salahub, D. R. *J. Chem. Phys.* **1994**, *101*, 7633–42.
- (138) Wei, D.; Salahub, D. R. *J. Chem. Phys.* **1997**, *106*, 6086–6094.
- (139) Schmidt, R. G.; Brickmann, J. *Ber. Bunsen-Ges. Phys. Chem.* **1997**, *101*, 1816–1827.
- (140) Pavese, M.; Voth, G. A. *Ber. Bunsen-Ges. Phys. Chem.* **1998**, *102*, 527–532.
- (141) Cheng, H.-P. *J. Phys. Chem. A* **1998**, *102*, 6201–6204.
- (142) Marx, D.; Tuckerman, M. E.; Hutter, J.; Parrinello *Nature* **1999**, *397*, 601–604.
- (143) Jiang, J.-C.; Wang, Y.-S.; Chang, H.-C.; Lin, S. H.; Lee, Y. T.; Niedner-Schatteburg, G.; Chang, H.-C. *J. Am. Chem. Soc.* **2000**, *122*, 1398–1410.
- (144) Misaizu, F.; Sanekata, M.; Fuke, K.; Iwata, S. *J. Chem. Phys.* **1994**, *100*, 1161–1170.
- (145) Sanekata, M.; Misaizu, F.; Fuke, K. *J. Chem. Phys.* **1996**, *104*, 9768–9778.
- (146) Peschke, M.; Blades, A. T.; Kebarle, P. *J. Phys. Chem. A* **1998**, *102*, 9978–9985.
- (147) Peschke, M.; Blades, A. T.; Kebarle, P. *Int. J. Mass Spectrom.* **1999**, *185*, 685–699.
- (148) Beyer, M.; Williams, E. R.; Bondybey, V. E. *J. Am. Chem. Soc.* **1999**, *121*, 1565–1573.
- (149) Agmon, N. *J. Phys. Chem. A* **1998**, *102*, 192–199.
- (150) Mactaylor, R. S.; Gilligan, J. J.; Moody, D. J.; Castleman, A. W., Jr. *J. Phys. Chem. A* **1999**, *103*, 2655–2658.
- (151) Mactaylor, R. S.; Gilligan, J. J.; Moody, D. J.; Castleman, A. W., Jr. *J. Phys. Chem. A* **1999**, *103*, 4196–4201.
- (152) Achatz, U.; Joos, S.; Berg, C.; Schindler, T.; Beyer, M.; Albert, G.; Niedner-Schatteburg, G.; Bondybey, V. E. *J. Am. Chem. Soc.* **1998**, *120*, 1876–1882.
- (153) Nicol, G.; Sunner, J.; Kebarle, P. *Int. J. Mass Spectrom. Ion Processes* **1988**, *84*, 135–155.
- (154) Schindler, T.; Berg, C.; Niedner-Schatteburg, G.; Bondybey, V. E. *Chem. Phys.* **1995**, *201*, 491–6.
- (155) Ferguson, E. E.; Fehsenfeld, F. C.; Albritton, D. L. In *Gas-Phase Ion Chemistry*; Bowers, M. T., Ed.; Academic Press: New York, 1979; Vol. 1.
- (156) Smith, D.; Adams, N. G. In *Gas Phase Ion Chemistry*; Bowers, M. T., Ed.; Academic Press: New York, 1979; Vol. 1.
- (157) Choi, J. H.; Kuwata, K. T.; Haas, B. M.; Cao, Y.; Jonsson, M. S.; Okumura, M. *J. Chem. Phys.* **1994**, *100*, 7153–65.
- (158) Angel, L.; Stace, A. J. *J. Phys. Chem. A* **1998**, *102*, 3037–3041.
- (159) Angel, L.; Stace, A. J. *J. Chem. Phys.* **1998**, *109*, 1713–1715.
- (160) Albritton, D. L.; Watson, R. T.; Aucamp, P. J. *Scientific Assessment of Ozone Depletion: 1994*; World Meteorological Organization: Geneva, Switzerland, 1994.
- (161) Schindler, T.; Berg, C.; Niedner-Schatteburg, G.; Bondybey, V. E. *J. Chem. Phys.* **1996**, *104*, 3998–4004.
- (162) Cao, Y.; Choi, J.-H.; Haas, B.-M.; Okumura, M. *J. Phys. Chem.* **1994**, *98*, 12176–85.
- (163) Stace, A. J.; Winkel, J. F.; Atrill, S. R. *J. Chem. Soc., Faraday Trans.* **1994**, *90*, 3469–70.
- (164) Wincel, H.; Mereand, E.; Castleman, A. W., Jr. *J. Phys. Chem. A* **1997**, *101*, 8248–8254.
- (165) Hanson, D. R.; Ravishankara, A. R. *J. Phys. Chem.* **1992**, *96*, 2682–2691.
- (166) Hanson, D. R. *J. Phys. Chem.* **1995**, *99*, 13059–13061.
- (167) Bianco, R.; Hynes, J. T. *J. Phys. Chem. A* **1998**, *102*, 309–314.
- (168) Bianco, R.; Gertner, B. J.; Hynes, J. T. *Ber. Bunsen-Ges. Phys. Chem.* **1998**, *102*, 518–526.
- (169) Bianco, R.; Hynes, J. T. *J. Phys. Chem. A* **1999**, *103*, 3797–3801.
- (170) Campagnola, P. J.; Cyr, D. M.; Johnson, M. A. *Chem. Phys. Lett.* **1991**, *181*, 206–12.
- (171) Posey, L. A.; DeLuca, M. J.; Campagnola, P. J.; Johnson, M. A. *J. Phys. Chem.* **1989**, *93*, 1178–81.
- (172) Niedner-Schatteburg, G. Habilitationsschrift, Technische Universität München, 1996.
- (173) Beyer, M.; Lammers, A.; Savchenko, E. V.; Niedner-Schatteburg, G.; Bondybey, V. E. *Phys. Chem. Chem. Phys.* **1999**, *1*, 2213–2221.
- (174) Rodriguez-Cruz, S. E.; Klassen, J. S.; Williams, E. R. *J. Am. Chem. Soc.* **1999**, in press.
- (175) Sena, M.; Riveros, J. M. *J. Phys. Chem. A* **1997**, *101*, 4384–4391.
- (176) Sena, M.; Riveros, J. M. *Rapid Commun. Mass Spectrom.* **1994**, *8*, 1031–4.
- (177) Bohme, D. K.; Mackay, G. I.; Tanner, S. D. *J. Am. Chem. Soc.* **1979**, *101*, 3724–3730.
- (178) Smith, D.; Adams, N. G.; Alge, E. *Planet Space Sci.* **1981**, *29*, 449.
- (179) Udseth, H.; Zmora, H.; Beuhler, R. J.; Friedman, L. *J. Phys. Chem.* **1982**, *86*, 612–617.
- (180) Zhang, X.; Castleman, A. W., Jr. *J. Chem. Phys.* **1994**, *101*, 1157–1164.
- (181) Yang, X.; Zhang, X.; Castleman, A. W., Jr. *Int. J. Mass Spectrom. Ion Proc.* **1991**, *109*, 339–354.
- (182) Yang, X.; Castleman, A. W., Jr. *J. Chem. Phys.* **1990**, *95*, 130–134.
- (183) Honma, K.; Sunderlin, L. S.; Armentrout, P. B. *Int. J. Mass Spectrom. Ion Processes* **1992**, *117*, 237–259.
- (184) Nelson, C. M.; Okumura, M. *J. Phys. Chem.* **1992**, *96*, 6112–6115.
- (185) VanDoren, J. M.; Viggiano, A. A.; Morris, R. A. *J. Am. Chem. Soc.* **1994**, *116*, 6957–6958.
- (186) Spanel, P.; Smith, D. *J. Phys. Chem.* **1995**, *99*, 15551–6.
- (187) Hiraoka, K.; Shoda, T.; Yamabe, S.; Ignacio, E. W. *J. Mass Spectrom. Soc. Jpn.* **1998**, *46*, 442–447.
- (188) Bell, A. J.; Giles, K.; Moody, S.; Watts, P. *Int. J. Mass Spectrom. Ion Processes* **1998**, *173*, 65–70.
- (189) Arnold, S. T.; Thomas, J. M.; Viggiano, A. A. *Int. J. Mass Spectrom.* **1998**, *179*, 243–251.
- (190) Thomas, J. M.; Viggiano, A. A. *J. Phys. Chem. A* **1999**, *103*, 2720–2722.
- (191) Plastringer, B.; Cohen, M. H.; Cowen, K. A.; Wood, D. A.; Coe, J. V. *J. Phys. Chem.* **1995**, *99*, 118–122.
- (192) Zhang, X.; Mereand, E. L.; Castleman Jr., A. W. *J. Phys. Chem.* **1994**, *98*, 3554–3557.
- (193) Fehsenfeld, F. C.; Mosesman, M.; Ferguson, E. E. *J. Chem. Phys.* **1971**, *55*, 2120–2125.
- (194) Viggiano, A. A.; Morris, R. A.; Deakyne, C. A.; Dale, F.; Paulson, J. F. *J. Phys. Chem.* **1990**, *94*, 8193–8197.
- (195) Viggiano, A. A.; Morris, R. A.; Deakyne, C. A.; Dale, F.; Paulson, J. F. *J. Phys. Chem.* **1991**, *95*, 3644–7.
- (196) Squires, R. R. *Int. J. Mass Spectrom. Ion Processes* **1992**, *117*, 565–600.
- (197) Paulson, J. F.; Dale, F. *J. Chem. Phys.* **1982**, *77*, 4006.
- (198) Hierl, P. M.; Paulson, J. F. *J. Chem. Phys.* **1984**, *80*, 4890.
- (199) Hierl, P. M.; Paulson, J. F.; Henchman, M. J. *J. Phys. Chem.* **1995**, *99*, 15655–15661.
- (200) Arnold, S. T.; Viggiano, A. A. *J. Phys. Chem. A* **1997**, *101*, 2859–2861.
- (201) Fahey, D. W.; Böhringer, H.; Fehsenfeld, F. C.; Ferguson, E. E. *J. Chem. Phys.* **1982**, *76*, 1799–1805.
- (202) Yang, X.; Castleman, A. W., Jr. *Chem. Phys. Lett.* **1991**, *179*, 361–6.
- (203) Wincel, H.; Mereand, E.; Castleman, A. W., Jr. *J. Phys. Chem.* **1995**, *99*, 6601–6607.
- (204) Wincel, H.; Mereand, E.; Castleman, A. W., Jr. *J. Phys. Chem.* **1996**, *100*, 7488–7493.
- (205) Wincel, H.; Mereand, E.; Castleman, A. W., Jr. *J. Phys. Chem.* **1996**, *100*, 16808–16816.
- (206) Mereand, E.; Wincel, H.; Castleman, A. W., Jr. *Int. J. Mass Spectrom.* **1999**, *182*, 31–44.
- (207) Wincel, H.; Mereand, E.; Castleman, A. W., Jr. *J. Chem. Phys.* **1995**, *102*, 9228–9234.
- (208) Wincel, H.; Mereand, E.; Castleman, A. W., Jr. *J. Phys. Chem.* **1995**, *99*, 15678–15685.
- (209) Blades, A. T.; Ho, Y.; Kebarle, P. *J. Am. Chem. Soc.* **1996**, *118*, 196–201.
- (210) Blades, A. T.; Ho, Y.; Kebarle, P. *J. Phys. Chem.* **1996**, *100*, 2443–6.
- (211) Lavrich, D. J.; Buntine, M. A.; Serxner, D.; Johnson, M. A. *J. Phys. Chem.* **1995**, *99*, 8453–8457.
- (212) Seeley, J. V.; Morris, R. A.; Viggiano, A. A. *J. Phys. Chem. A* **1997**, *101*, 4598–4601.
- (213) Seeley, J. V.; Morris, R. A.; Viggiano, A. A. *J. Phys. Chem.* **1996**, *100*, 15821–15826.
- (214) Achatz, U.; Wagner, R.; Joos, S.; Fox, B. S.; Niedner-Schatteburg, G.; Bondybey, V. E. Manuscript in preparation.

CR9900650